

# 1 Regulation of poplar isoprenoid biosynthesis by methylerythritol 2 phosphate and mevalonic acid pathways interactions

3  
4 Ali Movahedi<sup>1</sup>, Hui Wei<sup>1,†</sup>, Boas Pucker<sup>2,†</sup>, Weibo Sun<sup>1</sup>, Dawei Li<sup>1</sup>, Liming Yang<sup>1,\*</sup>, and Qiang  
5 Zhuge<sup>1,\*</sup>

6  
7 <sup>1</sup> Co-Innovation Center for Sustainable Forestry in Southern China, Key Laboratory of Forest  
8 Genetics & Biotechnology, Ministry of Education, College of Biology and the Environment,  
9 Nanjing Forestry University, Nanjing 210037, China; ali\_movahedi@njfu.edu.cn (A.M.);  
10 15850682752@163.com (H.W.); czswb@njfu.edu.cn (W.S.); dwli@njfu.edu.cn (D.L.);  
11 yangliming@njfu.edu.cn (L.Y.); qzhuge@njfu.edu.cn (Q.Z.)

12 <sup>2</sup> Institute of Plant Biology, TU Braunschweig, Braunschweig, Germany; b.pucker@tu-  
13 braunschweig.de (B.P.)

14  
15  
16 \* Correspondence: qzhuge@njfu.edu.cn; yangliming@njfu.edu.cn; Fax: +86-25-8542-8701

17  
18 † These authors contributed equally.

## 32 **Summary**

33 Plants use two distinct isoprenoid biosynthesis routes: methylerythritol phosphate (MEP) and  
 34 mevalonic acid (MVA) pathways. The rate-limiting enzymes of the MEP pathway are 1-deoxy-  
 35 D-xylulose5-phosphate synthase (DXS) and 1-deoxy-D-xylulose5-phosphate reductoisomerase  
 36 (DXR). 3-hydroxy-3-methylglutaryl-CoA reductase (HMGR) catalyzes the rate-limiting step in  
 37 the MVA pathway. Previously, overexpression of *Populus trichocarpa* *PtDXR* was found to  
 38 upregulate resistance against salt and drought stresses. We showed  
 39 while *PtHMGR* overexpressors (OEs) exhibited different MEP- and MVA-related gene  
 40 expressions than non-transgenic poplars (NT), the *PtDXR*-OEs revealed upregulated MEP-  
 41 related and downregulated MVA-related gene expressions. *PtDXR* and *PtHMGR*  
 42 overexpressions caused changes in MVA-derived trans-zeatin-riboside, isopentenyl adenosine,  
 43 castasterone, and 6-deoxocastasterone well as MEP-derived carotenoids and gibberellins.  
 44 In *PtHMGR*-OEs, the accumulated geranyl diphosphate synthase (*GPS*) and geranyl  
 45 pyrophosphate synthase (*GPPS*) transcript levels in the MEP pathway led to an accumulation  
 46 of MEP-derived isoprenoids. In contrast, upregulation of farnesyl diphosphate synthase (*FPS*)  
 47 expression in the MVA pathway contributed to increased levels of MVA-derived isoprenoids.  
 48 In addition, *PtHMGR*-OEs increased MEP-related *GPS* and *GPPS* transcript levels, expanded  
 49 MEP-derived isoprenoid levels, changed *FPS* transcript levels, and affected MVA-derived  
 50 isoprenoid yields. These results suggest that interaction exists between the MVA- and MEP-  
 51 pathways.

52 **Keywords:** MEP; MVA; poplar; terpenoids; Pathway interaction

53

54

55

56

57

58

59

60

61

62

## 63 1. Introduction

64 Plants terpenoids include gibberellins (GAs), carotene, Lycopene, cytokinins (CKs),  
 65 strigolactones (GRs), and brassinosteroids (BRs) are produced through methylerythritol  
 66 phosphate (MEP) and mevalonic acid (MVA) pathways (Henry et al., 2015; van Schie et al.,  
 67 2006; Xie et al., 2008). The mentioned pathways are involved in plant growth, development,  
 68 and response to environmental changes (Bouvier et al., 2005; Kirby and Keasling, 2009). The  
 69 isopentenyl diphosphate isomerase (IDI) catalyzes the conversion of the isopentenyl  
 70 diphosphate (IPP) into dimethylallyl diphosphate (DMAPP), leading to provide the basic  
 71 materials for all isoprenoid productions (Hemmerlin, 2012; Lu et al., 2012; Zhang et al., 2019).  
 72 The produced IPP and DMAPP play essential roles in MEP and MVA pathways interactions  
 73 (Huchelmann et al., 2014; Liao et al., 2016). The MVA pathway reactions appear in the  
 74 cytoplasm, endoplasmic reticulum (ER), and peroxisomes (Cowan et al., 1997; Roberts, 2007),  
 75 producing sesquiterpenoids and sterols. The 3-hydroxy-3-methylglutaryl-CoA reductase  
 76 (HMGR), a rate-limiting enzyme in the MVA pathway, catalyzes 3-hydroxy-3-methylglutary-  
 77 CoA (HMG-CoA) to form MVA (Cowan et al., 1997; Roberts, 2007).

78 Reactions of the MEP pathway occur in the chloroplast and produce carotenoids, GAs,  
 79 and diterpenoids. 1-deoxy-D-xylulose5-phosphate synthase (DXS) and 1-deoxy-D-xylulose5-  
 80 phosphate reductoisomerase (DXR) are rate-limiting enzymes in the MEP pathway that  
 81 catalyze the conversion of D-glyceraldehyde3-phosphate (D-3-P) and pyruvate into 2-C-  
 82 methyl-D-erythritol4-phosphate (MEP) (Cordoba et al., 2009; Perreca et al., 2020; Wang et al.,  
 83 2012; Yamaguchi, 2018). Terpenoids like phytoalexin and volatile oils play essential roles in  
 84 plant growth, development, and disease resistance (Hain et al., 1993; Ren et al., 2008).  
 85 Photosynthetic pigments convert organic carbon into plant biomass (Esteban et al., 2015). In  
 86 addition to an extensive range of natural functions in plants, terpenoids also consider the  
 87 potential for biomedical applications. Paclitaxel is one of the most effective chemotherapy  
 88 agents for cancer treatment, and artemisinin is an anti-malarial drug (Kim et al., 2016a; Kong  
 89 and Tan, 2015).

90 Previous metabolic engineering studies have proposed strategies to improve the  
 91 production of specific metabolites in plants (Ghirardo et al., 2014; Opitz et al., 2014). For  
 92 example, PMT and H6H encoding the putrescine N-methyltransferase and hyoscyamine 6  $\beta$ -

93 hydroxylase respectively produced significantly higher scopolamine in transgenic henbane  
94 hairy root. Also, HCHL encoding p-hydroxycinnamoyl-CoA hydratase/lyase accumulated the  
95 glucose ester of p-hydroxybenzoic acid (pHBA) in *Beta vulgaris* hairy root (Rahman et al., 2009;  
96 Zhang et al., 2004). The 3-hydroxy-3-methylglutaryl-coenzyme A synthase (HMGS) is the  
97 second enzyme in the MVA pathway. Liao et al. (2018) confirmed that *HMGS* overexpression  
98 of *Brassica juncea* upregulates carotenoid and phytosterol in tomatoes. HMGR has been  
99 considered a critical factor in metabolically engineering terpenoids (Aharoni et al., 2005;  
100 Dueber et al., 2009). In addition, *PgHMGR1* overexpression of ginseng increases ginsenosides  
101 content, which is a necessary pharmaceutically active component (Kim, 2014).

102 Transgenic tobacco overexpressing the *Hevea brasiliensis* *HMGR* enhanced the  
103 phytosterol levels (Schaller et al., 1995). It has been shown (Dai et al., 2011)  
104 that *SmHMGR2* in *Salvia miltiorrhiza*, resulting in the improvement of squalene and  
105 tanshinone contents. Moreover, *Arabidopsis thaliana* *HMGR1* (*AtHMGR1*) enhanced the  
106 phytosterol levels in the first generation of transgenic tomatoes (Enfissi et al., 2005). While  
107 the deaccumulation of *DXR* transcripts resulted in lower pigmentation and chloroplast  
108 appearance defects, the upregulated *DXR* expression caused the MEP-derived plastid  
109 isoprenoids to accumulate. Therefore, *DXR* can be genetically engineered to regulate the  
110 content of terpenoids and expressed *DXR* in *Arabidopsis* and observed enhanced flux through  
111 the MEP pathway (Carretero-Paulet et al., 2006). While the *A. thaliana* *DXR* overexpression  
112 caused the diterpene anthiolimine to accumulate in *Salvia sclarea* hairy roots (Vaccaro et al.,  
113 2014), the peppermint *DXR* overexpression resulted in essential oil inflation (about 50%) with  
114 no significant variations in monoterpene composition (Mahmoud and Croteau, 2001).  
115 Furthermore, previous studies have shown the exchange of metabolic intermediates included  
116 in the MVA- and MEP-pathways through plastid membranes (Laule, 2003; Liao, 2006). In  
117 summary, the overexpression of genes involved in the MEP- and MVA-pathways can change  
118 the abundances or activities of related enzymes and metabolic products, causing a new  
119 opportunity for plant breeding to enhance the accumulation of related metabolic products.

120 Poplars as an economic and energy species are widely used in industrial and agricultural  
121 production. Its fast growth characteristics and advanced resources in artificial afforestation  
122 play a vital role in the global ecosystem (Devappa, 2015).

123 This study investigates the poplar isoprenoid biosynthesis. We showed that *PtHMGR*-

*OEs* upregulated MVA- and MEP-related genes in the transcript levels. *PtDXR-OEs* have also been shown involved in MVA-related genes down-regulation and MEP-related genes up-regulation, resulting in increased terpenoid collection. These results indicate that the MEP is a dominant pathway interacting with the MVA pathway and *HMGR* and *DXR* genes play key regulation points in these pathways.

## 2. Results

### 2.1. Isolation of the *PtHMGR* and *PtDXR* genes and characterization of transgenic poplars

The amino acid sequence of *PtHMGR* (Potri.004G208500.1) contains domains of other HMGRs, including HMG-CoA-binding motifs (EMPVG YVQIP' and 'TTEGCLVA) and NADPH-binding motifs (DAMGMNMV' and 'VGTVGGGT) (Ma et al., 2012) (Supplemental Figure 1). Consequently, a phylogenetic tree with previously characterized HMGRs supported the *PtHMGR* candidate identification (Supplemental Figure 2). The open reading frame of the *PtHMGR* was amplified from *Populus trichocarpa* cDNA to clone in pEASY-T3 (TransGen Biotech, China) and sequencing. The putative transgenic lines showed amplicons in PCR identification compared to NT poplar (Supplemental Figure 3a). They also exhibited increased *PtHMGR-OEs* expressions than NT (Supplemental Figure 3b), indicating successful overexpression of *PtHMGR* in poplar. In addition, the *PtDXR* gene, which has been isolated, sequenced, and analyzed previously by the authors (Xu et al., 2019), was used as the *PtDXR-OEs* in this study.

### 2.2. Effects of *PtHMGR* and *PtDXR* overexpressions on MVA- and MEP-related gene expressions

MVA-related genes *AACT*, *MVK*, and *MVD* except *HMGS* were significantly upregulated in *PtHMGR-OE* transgenics than NT poplars (Figure 1a). While the expression of MEP-related genes *DXS*, *DXR*, 1-hydroxy-2-methyl-2-(E)-butenyl-4-diphosphate synthase (*HDS*), 1-hydroxy-2-methyl-2-(E)-butenyl-4-diphosphate reductase (*HDR*), *IDI*, and *GPPS* were significantly promoted in all *PtHMGR-OEs* transgenic poplars in comparing with NT, the *GPS* overexpression was enhanced only by *PtHMGR-OE3* (Figure 1b). In addition, 2-C-methyl-d-erythritol-4-phosphate cytidyltransferase (*MCT*) and 4-diphosphocytidyl-2-C-methyl-D-erythritol kinase (*CMK*) have been downregulated by *PtHMGR-OEs* (Figure 1b).

Moreover, while only *FPS* revealed significant upregulation by *PtDXR*-OEs in transgenics comparing with NT, the other MVA-related genes *AACT*, *HMGS*, *HMGR*, and *MVK* were considerably downregulated (Figure 1c). Finally, all MEP-related genes revealed significant upregulation in *PtDXR*-OEs transgenic poplars (Figure 1d). *GPPS* and *HDS* genes exposed more expressions induced by *DXR*-OEs than the other MEP-related genes (Figure 1d).

### 2.3. *PtHMGR overexpression influences the production of MVA and MEP derivatives*

$\beta$ -carotene is a carotenoid synthesis that has been broadly used in the industrial composition of pharmaceuticals and as food colorants, animal supplies additives, and nutraceuticals. MVA-and MEP-pathways have been proved that are effective in the biosynthesis of  $\beta$ -carotene (Yang, 2014). In addition, Lycopene is a carotenoid referring to C40 terpenoids and is broadly found in various plants, particularly vegetables and fruits. It has been shown that MVA and MEP-pathways directly influence the biosynthesis production of Lycopene (Kim et al., 2019; Wei et al., 2018). While Wille et al. (2004) showed that  $\beta$ -carotene and Lutein are synthesized using intermediates from the MEP pathway, Opitz et al. (2014) revealed that both MVA and MPE pathways contribute to producing isoprenoids such as  $\beta$ -carotene and Lutein. HPLC-MS/MS has analyzed the quantity of MVA and MEP derivatives. Our analyses revealed that *HMGR*-OEs caused a significant enhancement in Lycopene (an average of ~ 0.08 ug/g),  $\beta$ -carotene (an average of ~ 0.33 ug/g), and Lutein (an average of ~ 272 ug/g) production compared with NT poplars (~0.02, ~0.08, and ~100 ug/g respectively) (Figure 2a, b, and c; Supplementary Figure 4). The ABA-related gene expressions also have been calculated. Results revealed significant increased of *ZEP1*, 2, and 3 relative gene expressions with the averages of ~2.85, ~4.67, and ~2.92 compared to NT with an average of ~1 (Figure 2d). These results also shown meaningful enhancements of *NCED1*, 2, and 3 relative gene expressions with the averages of ~4.16, ~3.79, and ~3.4 compared to NT with an average of ~1 (Figure 2e).

### 2.4. *Enhanced carotenoid levels in PtDXR-OE poplars*

The levels of the MEP-derived substances lycopene,  $\beta$ -carotene, and Lutein were significantly increased in *PtDXR*-OEs with the averages of ~0.08, 0.22, 209.32 ug/g, respectively compared to NT poplars (Figure 3a, b, and c; Supplemental figure 5). The analyses

of ABA-related gene expressions revealed significantly increased *ZEP1*, 2, and 3 relative gene expressions with the averages of ~2.63, ~2.38, and ~3.86 compared to NT with an average of ~1 (Figure 3d). These results also showed meaningful enhancements of *NCED2* and 3 relative gene expressions with averages of ~2.25 and ~2.21 compared to NT with an average of ~1 (Figure 2e). These results revealed a decreased average in *NCED1* relative gene expression with an average of ~0.66 compared to NT poplars.

## 2.5. Other MVA and MEP derivatives

The other MVA and MEP derivatives such as GAs, trans-zeatin-riboside (tZR), isopentenyl adenosine (IPA), 6-deoxyocastasterone (DCS), and castasterone (CS) productions affected by *PtHMGR*- and *PtDXR*-OEs have been analyzed. While Gibberellic acid (GA3) (a downstream product of MEP) (an average of ~0.22 ng/g), tZR (an average of ~0.06 ng/g), IPA (an average of ~0.59 ng/g), DCS (an average of 4.95 ng/g) revealed significantly more productions induced by *HMGR*-OEs, the CS production (~0.095 ng/g) was decreased considerably compared to NT poplars (~0.10, ~0.03, ~0.37, ~1.50, and ~0.20 ng/g respectively) (Figure 4a-j). These results demonstrate that the *HMGR* gene interacts with MVA and MEP derivatives productions in plants. On the other hand, the *PtDXR* overexpression significantly affected the contents of MEP- and MVA-derived products except for CS. *PtDXR*-OEs showed a significant increase ~0.276 ng/g in the GA3 content (Figure 4a and f). The tZR content represented a 10-fold increase (~0.304 ng/g) affected by *PtDXR*-OEs compared to NT poplars (0.032 ng/g) (Figure 4b and g). The content of IPA in *PtDXR*-OEs meaningfully increased ~ 0.928 ng/g, compared to 0.363 ng/g in NT poplars (Figure 4c and h) with a 3-fold increase. In addition, the DCS content considerably increased to ~3.36 ng/g, comparing with ~1.50 ng/g in NT, representing a 3-fold increase in *PtDXR*-OEs (Figure 4d and i). By contrast, the content of CS in *PtDXR*-OEs significantly decreased (~0.137 ng/g) compared to NT poplar (0.203 ng/g), indicating significant down-regulation in *PtDXR*-OEs (Figure 4e and j). The HPLC-MS/MS chromatograms of GA, tZR, IPA, DCS, and CS standards are provided in Supplemental Figures 6–10.

## 2.6. Phenotypic properties

To figure out the effect of MVA-and MEP-pathway interactions and their changes by *PtHMGR*- and *PtDXR*-OEs on plant growth and development, we decided to evaluate



phenotypic changes. Our results revealed a significant increase in GA3 contents in *PtDXR*-*OEs* (Figure 4a) associated with a considerable rise in cytokinin tZR (Figure 4b), resulting in significantly more development in stem length compared to *PtHMGR*-*OEs* and NT poplars (Figure 5a and d). Regarding increasing ABA-related genes (*ZEP* and *NCED*) in *PtHMGR*-*OEs* than *PtDXR*-*OEs* and NT poplars (Figure 5b) and also concerning insufficient increase cytokinin tZR in *PtHMGR*-*OEs* comparing with NT poplars (Figure 4b), *PtHMGR* transgenics showed a shorter stem length than *PtDXR* transgenics compared with NT poplars (Figure 5d). We also figured out that only *PtDXR*-*OEs* revealed a few significant increases in stem diameters than *PtHMGR*-*OEs* and NT poplars (Figure 5c and d).

### 3. Discussion

#### 3.1. Characterization and evolutionary history of *HMGR*

Expression domains of *HMGR1* and *HMGR2* indicate a subfunctionalization. The expression of *CaHMGR1* is temporary and tissue-specific, whereas that of *CaHMGR2* is constitutive. *CaHMGR1* is only expressed in fruit tissues (pulp, endosperm, endocarp), flower buds, and leaves during the initial developing steps. In contrast, *CaHMGR2* is expressed in all tissues (flower buds, leaves, branches, and roots) and fruit tissues at various developing steps (Tiski et al., 2011). *LcHMGR1* is most highly expressed during the early stages of fruit development and regulates fruit size. The expression level of *LcHMGR1* is higher, and expression lasts longer in larger fruits. *LcHMGR2* shows an expression peak during the late stages of fruit development and is related to the biosynthesis of isoprenoid substances required for cell elongation during that time (Rui et al., 2012). Previous studies have shown that *NtHMGR2* is a stress-responsive gene (Hemmerlin et al., 2004; Merret et al., 2007). In this study, high similarity of *PtHMGR* with other known *HMGR1* was observed. Because *HMGR* is a conserved gene with a vital function in the MVA pathway, it can be used as a reference gene to determine relationships among species.

#### 3.2. *HMGR* overexpression results in upregulation of isoprenoid biosynthesis gene expression

Liao et al. (2018) showed that overexpression of *BjHMGS1* affects the expression levels of MEP- and MVA-related genes and slightly increases the transcript levels of *DXS* and *DXR* in



transgenic plants. However, *DXS*, *DXR*, *HDS*, and *HDR* expression levels have been improved significantly in *PtHMGR-OE* poplars, while *MCT* and *CMK* are downregulated.

Similar to Liao et al. (2018) which the *BjHMGS1* overexpression in tomatoes significantly increased the *GPS* and *GPPS* expressions, we exhibited that the *PtHMGR* overexpression enhanced the farnesyl diphosphate synthase (*FPS*), *GPS*, and *GPPS* expressions may stimulate the interaction between IPP and DMAPP, increasing the biosynthesis of plastidial C15 and C20 isoprenoid precursors. Xu et al. (2012) showed that *HMGR* overexpression in *Ganoderma lucidum* caused upregulated *FPS*, squalene synthase (*SQS*), or lanosterol synthase (*LS*) mRNA expressions and developed the contents of ganoderic acid and intermediates, including squalene and lanosterol. In addition, the *BjHMGS1* overexpression in tomatoes significantly increased transcript levels of *FPS*, *SQS*, squalene epoxidase (*SQE*), and cycloartenol synthase (*CAS*) (Liao et al., 2018). This study exhibited that except for *HMGS* downregulating, the *AACT*, *MVK*, and *MVD* transcript levels were significantly upregulated in *PtHMGR-OE* poplars. We revealed that these enhanced gene expressions mainly were associated with the MVA-related genes contributing to the biosynthesis of sesquiterpenes and other C15 and universal C20 isoprenoid precursors.

### 3.3. Overexpression of *PtDXR* affects MEP- and MVA-related genes

Zhang et al. (2018) showed that the *TwDXR* overexpression in *Tripterygium wilfordii* increases the *TwHMGS*, *TwHMGR*, *TwFPS*, and *TwGPPS* expressions but decreases the *TwDXS* expression. Moreover, Zhang et al. (2015) exhibited that the *NtDXR1* overexpression in tobacco increases the transcript levels of eight MEP-related genes, indicating that the *NtDXR1* overexpression led to upregulated MEP-related gene expressions. In *A. thaliana*, the *DXR* transcript level changes do not affect *DXS* gene expression or enzyme accumulation, although the *DXR* overexpression promotes MEP-derived isoprenoids such as carotenoids, chlorophylls, and taxadiene (Carretero-Paulet et al., 2006).

On the other hand, the potato *DXS* overexpression in *A. thaliana* led to upregulation of downstream *GGPPS* and phytoene synthase (*PSY*) genes (Henriquez et al., 2016). Furthermore, (Simpson et al., 2016) exhibited that the *A. thaliana DXS* overexpression in *Daucus carota* caused to enhance the *PSY* expression significantly.

In this study, while the *PtDXR-OEs* exposed higher MEP-related gene expressions than NT

poplars, the *PtDXR-OEs* revealed significant downregulated MVA-related gene expressions than NT poplars. These findings illustrate that the MEP pathway regulates monoterpenes, diterpenes, and tetraterpenoids biosynthesis and could affect the MVA pathway.

The diversity of biosynthetic pathways, the complexity of metabolic networks, and the insufficient knowledge of gene regulation led to species-specific regulation patterns of MEP- and MVA-related gene expression. One possible conclusion is that MEP- and MVA-related genes often do not work alone but are co-expressed with upstream and downstream genes in the MEP- and MVA- pathways to carry out a specific function.

### 3.4. *Overexpression of HMGR promotes the formation of GAs, and carotenoids in plastids and accumulation of tZR, IPA, and DCS in the cytoplasm*

HMGR, as the rate-limiting enzyme in the MVA-pathway of plants, plays a critical role in controlling the flow of carbon within this metabolic pathway. The upregulation of *HMGR* significantly increases isoprenoid levels in plants. Overexpression of *HMGRs* of different plant species has been reported to raise isoprenoids levels significantly. The heterologous expression of *Hevea brasiliensis HMGR1* in tobacco increased the sterol content and accumulated intermediate metabolites (Schaller et al., 1995). The *A. thaliana HMGR* overexpression in *Lavandula latifolia* increased the levels of sterols in the MVA- and MEP-derived monoterpenes and sesquiterpenes (Munoz-Bertomeu et al., 2007). In addition, the *Salvia miltiorrhiza SmHMGR* overexpression in hairy roots developed MEP-derived diterpene tanshinone (Kai et al., 2011). In our study, ABA synthesis-related genes (*NCED1*, *NCED3*, *NCED6*, *ZEP1*, *ZEP2*, and *ZEP3*) and the contents of GA3 and carotenoids were upregulated in *PtHMGR-OE* poplar seedlings. This finding suggests that the *HMGR* overexpression may indirectly affect the biosynthesis of MEP-related isoprenoids, including GA3 and carotenoids. The accumulation of MVA-derived isoprenoids including tZR, IPA, and DCS was significantly elevated in *PtHMGR-OEs*, indicating that *PtHMGR* overexpression directly influences the biosynthesis of MVA-related isoprenoids. Therefore, the *HMGR* gene directly affects MVA-derived isoprenoids and indirectly affects the content of MEP-derived isoprenoids by changing the expression levels of MEP-related genes.

### 3.5. *Higher levels of MEP- and MVA-derived products in PtDXR-OE seedlings*

DXR is the rate-limiting enzyme in the MEP pathway and an essential regulatory step in

the cytoplasmic metabolism of isoprenoid compounds (Takahashi et al., 1998). Mahmoud and Croteau (2001) revealed that overexpression of *DXR* in *Mentha piperita* promoted the synthesis of monoterpenes in the oil glands and increased the production of essential oil yield by 50%. However, the up-regulation of *DXR* expression did not lead to change in the complex oil composition significantly. Hasunuma et al. (2008) exhibited that overexpression of *Synechocystis* sp. strain PCC6803 *DXR* in tobacco resulted in increased levels of  $\beta$ -carotene, chlorophyll, antheraxanthin, and Lutein. Xing et al. (2010) showed that the *A. thaliana dxr* mutants caused to lack of GAs, ABA, and photosynthetic pigments (REF57). These mutants showed pale sepals and yellow inflorescences (Xing et al., 2010). In our study, the relatively higher abundance of GA3 and carotenoids in *PtDXR-OE* poplar seedlings indicated an effect of *DXR* overexpression. Combined with the result described above of increased *DXS*, *HDS*, *HDR*, *MCT*, *CMK*, *FPS*, *GPS*, and *GPPS* expression levels, we postulate that overexpression of *DXR* not only affects the expression levels of MEP-related genes but also changes the field of GA3, and carotenoids.

### 3.6. Interaction between the MVA and MEP pathways

Although the substrates of MVA- and MEP-pathways differ, there are common intermediates like IPP and DMAPP (Figure 6). Blocking only the MVA or the MEP pathway, respectively, does not entirely prevent the biosynthesis of terpenes in the cytoplasm or plastids, indicating that some MVA and MEP pathways products can be transported and/or move between cell compartments (Aharoni et al., 2003; Aharoni et al., 2004; Gutensohn et al., 2013). For example, it has been shown that the transferring IPP from the chloroplast to cytoplasm observed through <sup>13</sup>C labeling, indicating that plentiful IPP is available for use in the MVA-pathway to produce terpenoids (Ma et al., 2017). In addition, segregation between the MVA- and MEP-pathways is limited and might exchange some metabolites over the plastid membrane (Laule, 2003). Kim et al. (2016b) used clustered, regularly interspaced short palindromic repeats (CRISPR) technology to reconstruct the lycopene synthesis pathway and control the flow of carbon in the MEP-and MVA-pathways. The results showed that the expression of MVA-related genes was reduced by 81.6%, but the lycopene yield was significantly increased. By analyzing gene expression levels and metabolic outcome in *PtHMGR*-and *PtDXR-OEs*, we discovered that the correlation might exist between MVA- and

MEP-related genes with MVA- and MEP-derived products, which are not restricted to crosstalk between IPP and DMAPP (Figure 6).

On the one hand, overexpression of *PtDXR* affected the transcript levels of MEP-related genes and the contents of MEP-derived isoprenoids, including GAs and carotenoids. The diminished accumulation of MVA-related gene products causes a reduction in the yields of MVA-derived isoprenoids (including CS) but leads to increasing tZR, IPA, and DCS contents. We hypothesize that IPP and DMAPP produced by the MEP pathway could enter the cytoplasm to compensate for the lack of IPP and DMAPP, and the IPP and DMAPP as the precursors of the MVA pathway are used to guide the synthesis of MVA-derived products. On the other hand, *PtHMGR-OEs* exhibited higher transcript levels of *AACT*, *MVK*, and *MVD* and higher *DXS*, *DXR*, *HDS*, and *HDR* than NT poplars, resulting in effect both MEP- and MVA-related gene expressions. We successfully demonstrated that manipulation of *HMGR* in the poplar MVA-pathway results in dramatically enhanced yields of GAs and carotenoids. This result illustrates that cytosolic *HMGR* overexpression expanded plastidial GPP- and GGPP-derived products, such as carotenoids. Therefore, this study provides hints that crosstalk between the MVA- and MEP-pathways increased the expression levels of *GPS* and *GPPS* in *PtHMGR-OEs*, and elevated the contents of GA3 and carotenoids. Moreover, changes in MEP- and MVA-related gene expressions affect MVA- and MEP-derived isoprenoids. Identification of the molecular mechanism holding this crosstalk requires further investigation.

In conclusion, overexpression of *PtHMGR* in poplars caused the accumulation of MVA-derived isoprenoids and MEP-derived substances. The advanced insights into the regulation of MVA- and MEP-pathways in poplar add to the knowledge about these pathways in Arabidopsis, tomato, and rice. In *PtHMGR-OE* poplars, most MEP- and MVA-related genes associated with the biosynthesis of isoprenoid precursors were upregulated. In *PtDXR-OE* poplars, elevated contents of GAs, carotenoids, and GRs were attributed to increased expression of MEP-related genes as well as plastidial *GPP* and *GGPP*. Together, these results show that manipulating *PtDXR* and *PtHMGR* is a novel strategy to influence poplar isoprenoids.

### 3.7. *The impressed crosstalk between MVA- and MEP-pathways by PtHMGR- and PtDXR-OEs influence plant growth and developments*

It has been shown that Absciscic acid (ABA) and GA3 perform essential functions in cell division, shoot growth, and flower induction (Xing et al., 2016). It has also been demonstrated that the cytokinin tZR, a variety of phytohormones, perform a crucial function as root to shoot signals, directing numerous developmental and growth processes in shoots (Abul et al., 2010; Sakakibara, 2006). Regarding these findings, we showed how the interactions between MVA- and MEP-pathways and their changes affected by some stimulators (*HMGR*- and *DXR*-OEs) influenced plant growth, especially in stem length. Finally, We figured out that the gibberellic acid and cytokinin may be more effective in plant growth than inhibiting by ABA, causing higher *PtDXR*-OEs than *PtHMGR*-OEs compared with NT poplars.

## 4. Materials and Methods

### 4.1. *Plant materials and growth conditions*

Non-transgenic *P. trichocarpa* and *Populus × euramericana* cv. 'Nanlin 895' plants were cultured in half-strength Murashige and Skoog (1/2 MS) medium (pH 5.8) under conditions of 24°C and 74% humidity (Movahedi et al., 2015). Subsequently, NT and transgenic poplars were cultured in 1/2 MS under long-day conditions (16 h light/8 h dark) at 24°C for 1 month (Movahedi et al., 2018).

### 4.2. *PtHMGR and PtDXR genes isolation and vector construction*

To produce cDNA, total RNA was extracted from *P. trichocarpa* leaves and processed with PrimeScript™ RT Master Mix, a kind of reverse transcriptase (TaKaRa, Japan). Forward and reverse primers (Supplemental Table 1: *PtHMGR*-F and *PtHMGR*-R) were designed, and the open reading frame (ORF) of *PtHMGR* was amplified via PCR. We then used the total volume of 50µl including 2 µl primers, 2.0 µl cDNA, 5.0 µl 10 × PCR buffer (Mg<sup>2+</sup>), 4µl dNTPs (2.5 mM), 0.5 µl rTaq polymerase (TaKaRa, Japan) for the following PCR reactions: 95°C for 7 min, 35 cycles of 95°C for 1 min, 58°C for 1 min, 72°C for 1.5 min, and 72°C for 10 min. Subsequently, the product of the *PtHMGR* gene was ligated into the pEASY-T3 vector (TransGen Biotech, China) based on blue-white spot screening, and the *PtHMGR* gene was inserted into the vector pGWB9 (Song et al., 2016) using Gateway technology (Invitrogen, USA). On the other hand, all

steps to generate cDNA, RNA extraction, PCR, pEASY-T3 ligation, and vector construction (pGWB9-PtDXR) of *PtDXR* have been carried out according to Xu et al. (2019).

### 4.3. *Creation of phylogenetic tree*

We applied the ClustalX for multiple sequence alignment of HMGR proteins, and MEGA5.0 software was used to construct a phylogenetic tree using 1000 bootstrap replicates. The amino acid sequences of HMGR from *Populus trichocarpa*, *Arabidopsis thaliana*, *Gossypium raimondii*, *Malus domestica*, *Manihot esculenta*, *Oryza sativa*, *Prunus persica*, *Theobroma cacao*, and *Zea mays* were obtained from the National Center for Biotechnology Information database (<https://www.ncbi.nlm.nih.gov/>) and Phytozome (<https://phytozome-next.jgi.doe.gov/>).

### 4.4. *Transgenic poplars: generation and confirmation*

*Agrobacterium tumefaciens* var. EHA105 was used for the infection of poplar leaves and petioles (Movahedi et al., 2014). Poplar buds were screened on differentiation MS medium supplemented with 30 µg/mL Kanamycin (Kan). Resistant buds were planted in bud elongation MS medium containing 20 µg/mL Kan and transplanted into 1/2 MS medium including 10 µg/mL Kan to generate resistant poplar trees. Genomic DNA has been extracted from putative transformants one-month-old leaves grown on a kanamycin-containing medium using TianGen kits (TianGen BioTech, China). The quality of the extracted genomic DNA (250–350 ng/µl) was determined by a BioDrop spectrophotometer (UK). PCR was carried out using designed primers (Supplementary Table 1: CaMV35S as the forward and PthMGR as the reverse), Easy Taq polymerase (TransGene Biotech), and 50 ng of extracted genomic DNA as a template to amplify about 2000 bp. In addition, total RNA was extracted from these one-month-old leaves to produce cDNA, as mentioned above. These cDNA then were applied to reverse transcription-quantitative PCR (RT-qPCR) (Supplemental Table 1: PthMGR forward and reverse) for comparing the transformants *PthMGR-OEs* expressions with NT poplars and transforming confirmation.

### 4.5. *Phenotypic properties evaluation*

To evaluate phenotypic changes, we selected 45-day-old poplars from PthMGR-and



PtDXR-OEs and NT poplars. We then simultaneously calculated the stem lengths (mm) and stem diameters (mm) every day and recorded them. All recorded were analyzed by GraphPad Prism 9, applying ANOVA one way (Supplemental Table 2).

#### 4.6. Analyses via qRT-PCR

12-month-old *PtDXR-OEs* (Xu et al., 2019) and *PtHMGR-OE* poplars (Soil-grown poplars) have been used to extract total RNA. The qRT-PCR was performed to identify MVA- and MEP-related gene expression levels in NT, *PtDXR-OE*, and *PtHMGR-OE* poplars. The qRT-PCR was served with a StepOne Plus Real-time PCR System (Applied Biosystems, USA) and SYBR Green Master Mix (Roche, Germany). Poplar *Actin* (*PtActin*) (XM-006370951.1) was previously tested as a reference gene for this experiment (Zhang et al., 2013). The following conditions were used for qRT-PCR reactions: pre-denaturation at 95°C for 10 min, 40 cycles of denaturation at 95°C for 15 s, and a chain extension at 60°C for 1 min. Three independent experiments were conducted using gene-specific primers (Supplemental Table 1: *PtHMGR* forward and reverse).

#### 4.7. Metabolite analyses via high-performance liquid chromatography-tandem mass spectrometry

The isopropanol/acetic acid extraction method extracted poplar endogenous hormones from NT, *PtDXR-OE*, and *PtHMGR-OE* leaves. GAs and CKs were extracted from, and then HPLC-MS/MS (Qtrap6500, Agilent, USA) was used to quantify levels of GAs, zeatin, tZR, and IPA. Also, methanol considered as solvent was used to extract 5-Deoxystrigol (5-DS), CS, and DCS, and HPLC-MS/MS (Agilent1290, AB; SCIEX-6500Qtrap, Agilent; USA) was also used to determine the contents of 5-DS, CS, and DCS. In addition, acetone, as a solvent, was used to isolate the carotenoid component of poplar leaves. To identify the carotenoid contents, the peak areas of carotenoids analyzed by HPLC (Symmetry Shield RP18, Waters, USA) were used to draw standard carotenoid curves, including  $\beta$ -carotene, Lycopene, and Lutein. Also, the HPLC was used to determine the contents of carotenoids, including  $\beta$ -carotene, Lycopene, and Lutein in NT and OE lines.

#### Author contributions

A.M. and H.W. conceived, planned, and coordinated the project, performed data analysis, wrote the draft, and finalized the manuscript. B.P. validated and contributed to data analysis and curation, revised and finalized the manuscript. W.S. and D.L. reviewed and edited the



manuscript. L.Y. and Q.Z. coordinated, contributed to data curation, finalized and funded this research. A.M., H.W., and B.P. contributed equally as the first author.

## Conflict of interest

The authors declare that they have no conflict of interest.

## Acknowledgments

This work was supported by the National Key Program on Transgenic Research (2018ZX08020002), the National Science Foundation of China (No. 31570650), and the Priority Academic Program Development of Jiangsu Higher Education Institutions.

## 5. Reference

- Abul, Y., Menendez, V., Gomez-Campo, C., Revilla, M.A., Lafont, F. and Fernandez, H. (2010) Occurrence of plant growth regulators in *Psilotum nudum*. *J Plant Physiol* **167**, 1211-1213.
- Aharoni, A., Giri, A.P., Deuerlein, S., Griepink, F., de Kogel, W.J., Verstappen, F.W., Verhoeven, H.A., Jongsma, M.A., Schwab, W. and Bouwmeester, H.J. (2003) Terpenoid metabolism in wild-type and transgenic *Arabidopsis* plants. *Plant Cell* **15**, 2866-2884.
- Aharoni, A., Giri, A.P., Verstappen, F.W., Berteau, C.M., Sevenier, R., Sun, Z., Jongsma, M.A., Schwab, W. and Bouwmeester, H.J. (2004) Gain and loss of fruit flavor compounds produced by wild and cultivated strawberry species. *Plant Cell* **16**, 3110-3131.
- Aharoni, A., Jongsma, M.A. and Bouwmeester, H.J. (2005) Volatile science? Metabolic engineering of terpenoids in plants. *Trends Plant Sci* **10**, 594-602.
- Bouvier, F., Rahier, A. and Camara, B. (2005) Biogenesis, molecular regulation and function of plant isoprenoids. *Prog Lipid Res* **44**, 357-429.
- Carretero-Paulet, L., Cairo, A., Botella-Pavia, P., Besumbes, O., Campos, N., Boronat, A. and Rodriguez-Concepcion, M. (2006) Enhanced flux through the methylerythritol 4-phosphate pathway in *Arabidopsis* plants overexpressing deoxyxylulose 5-phosphate reductoisomerase. *Plant Mol Biol* **62**, 683-695.
- Cordoba, E., Salmi, M. and Leon, P. (2009) Unravelling the regulatory mechanisms that modulate the MEP pathway in higher plants. *J Exp Bot* **60**, 2933-2943.
- Cowan, A.K., Moore-Gordon, C.S., Bertling, I. and Wolstenholme, B.N. (1997) Metabolic Control of Avocado Fruit Growth (Isoprenoid Growth Regulators and the Reaction Catalyzed by 3-Hydroxy-3-Methylglutaryl Coenzyme A Reductase). *Plant Physiol* **114**, 511-518.
- Dai, Z., Cui, G., Zhou, S.F., Zhang, X. and Huang, L. (2011) Cloning and characterization of a novel 3-hydroxy-3-methylglutaryl coenzyme A reductase gene from *Salvia miltiorrhiza* involved in diterpenoid tanshinone accumulation. *J Plant Physiol* **168**, 148-157.
- Devappa, R.K., Rakshit, S.K., Dekker, R.F., (2015) Forest biorefinery: Potential of poplar phytochemicals as value-added co-products. *Biotechnol Adv* **33**, 681-716.
- Dueber, J.E., Wu, G.C., Malmirchegini, G.R., Moon, T.S., Petzold, C.J., Ullal, A.V., Prather, K.L. and Keasling, J.D. (2009) Synthetic protein scaffolds provide modular control over metabolic flux. *Nat Biotechnol* **27**, 753-759.
- Enfissi, E.M., Fraser, P.D., Lois, L.M., Boronat, A., Schuch, W. and Bramley, P.M. (2005) Metabolic engineering of the mevalonate and non-mevalonate isopentenyl diphosphate-forming pathways for the production of health-promoting isoprenoids in tomato. *Plant Biotechnol J* **3**, 17-27.
- Esteban, R., Barrutia, O., Artetxe, U., Fernandez-Marin, B., Hernandez, A. and Garcia-Plazaola, J.I. (2015)

487 Internal and external factors affecting photosynthetic pigment composition in plants: a meta-analytical  
488 approach. *New Phytol* **206**, 268-280.

489 Ghirardo, A., Wright, L.P., Bi, Z., Rosenkranz, M., Pulido, P., Rodriguez-Concepcion, M., Niinemets, U.,  
490 Bruggemann, N., Gershenzon, J. and Schnitzler, J.P. (2014) Metabolic flux analysis of plastidic  
491 isoprenoid biosynthesis in poplar leaves emitting and nonemitting isoprene. *Plant Physiol* **165**, 37-51.

492 Gutensohn, M., Orlova, I., Nguyen, T.T., Davidovich-Rikanati, R., Ferruzzi, M.G., Sitrit, Y., Lewinsohn, E.,  
493 Pichersky, E. and Dudareva, N. (2013) Cytosolic monoterpene biosynthesis is supported by plastid-  
494 generated geranyl diphosphate substrate in transgenic tomato fruits. *Plant J* **75**, 351-363.

495 Hain, R., Reif, H.J., Krause, E., Langebartels, R., Kindl, H., Vornam, B., Wiese, W., Schmelzer, E., Schreier, P.H.,  
496 Stocker, R.H. and et al. (1993) Disease resistance results from foreign phytoalexin expression in a novel  
497 plant. *Nature* **361**, 153-156.

498 Hasunuma, T., Takeno, S., Hayashi, S., Sendai, M., Bamba, T., Yoshimura, S., Tomizawa, K., Fukusaki, E. and  
499 Miyake, C. (2008) Overexpression of 1-Deoxy-D-xylulose-5-phosphate reductoisomerase gene in  
500 chloroplast contributes to increment of isoprenoid production. *J Biosci Bioeng* **105**, 518-526.

501 Hemmerlin, A., Gerber, E., Feldtrauer, J.F., Wentzinger, L., Hartmann, M.A., Tritsch, D., Hoeffler, J.F., Rohmer,  
502 M. and Bach, T.J. (2004) A review of tobacco BY-2 cells as an excellent system to study the synthesis  
503 and function of sterols and other isoprenoids. *Lipids* **39**, 723-735.

504 Hemmerlin, A., Harwood, J. L., & Bach, T. J. (2012) A raison d'être for two distinct pathways in the early steps  
505 of plant isoprenoid biosynthesis? *Prog. Lipid Res.* **51**, 95-148.

506 Henriquez, M.A., Soliman, A., Li, G., Hannoufa, A., Ayele, B.T. and Daayf, F. (2016) Molecular cloning,  
507 functional characterization and expression of potato (*Solanum tuberosum*) 1-deoxy-d-xylulose 5-  
508 phosphate synthase 1 (StDXS1) in response to *Phytophthora infestans*. *Plant Sci* **243**, 71-83.

509 Henry, L.K., Gutensohn, M., Thomas, S.T., Noel, J.P. and Dudareva, N. (2015) Orthologs of the archaeal  
510 isopentenyl phosphate kinase regulate terpenoid production in plants. *Proc Natl Acad Sci U S A* **112**,  
511 10050-10055.

512 Huchelmann, A., Gastaldo, C., Veinante, M., Zeng, Y., Heintz, D., Tritsch, D., Schaller, H., Rohmer, M., Bach,  
513 T.J. and Hemmerlin, A. (2014) S-carvone suppresses cellulase-induced capsidiol production in *Nicotiana*  
514 *tabacum* by interfering with protein isoprenylation. *Plant Physiol* **164**, 935-950.

515 Kai, G., Xu, H., Zhou, C., Liao, P., Xiao, J., Luo, X., You, L. and Zhang, L. (2011) Metabolic engineering  
516 tanshinone biosynthetic pathway in *Salvia miltiorrhiza* hairy root cultures. *Metab Eng* **13**, 319-327.

517 Kim, M.J., Noh, M.H., Woo, S., Lim, H.G. and Jung, G.Y. (2019) Enhanced Lycopene Production in *Escherichia*  
518 *coli* by Expression of Two MEP Pathway Enzymes from *Vibrio* sp. *Dhg. Catalysts* **9**.

519 Kim, M.S., Haney, M.J., Zhao, Y., Mahajan, V., Deygen, I., Klyachko, N.L., Inskoe, E., Piroyan, A., Sokolsky, M.,  
520 Okolie, O., Hingtgen, S.D., Kabanov, A.V. and Batrakova, E.V. (2016a) Development of exosome-  
521 encapsulated paclitaxel to overcome MDR in cancer cells. *Nanomedicine* **12**, 655-664.

522 Kim, S.K., Han, G.H., Seong, W., Kim, H., Kim, S.W., Lee, D.H. and Lee, S.G. (2016b) CRISPR interference-  
523 guided balancing of a biosynthetic mevalonate pathway increases terpenoid production. *Metab Eng* **38**,  
524 228-240.

525 Kim, Y.J., Lee, O. R., Ji, Y. O., Jang, M. G., & Yang, D. C. (2014) Functional analysis of HMGR encoding genes  
526 in triterpene saponin-producing *Panax ginseng* Meyer. *Plant Physiol* **165**, 373-387.

527 Kirby, J. and Keasling, J.D. (2009) Biosynthesis of plant isoprenoids: perspectives for microbial engineering.  
528 *Annu Rev Plant Biol* **60**, 335-355.

529 Kong, L.Y. and Tan, R.X. (2015) Artemisinin, a miracle of traditional Chinese medicine. *Nat Prod Rep* **32**, 1617-  
530 1621.

531 Laule, O., Fürholz, A., Chang, H. S., Zhu, T., Wang, X., Heifetz, P. B., ... & Lange, M. (2003) Crosstalk between  
532 cytosolic and plastidial pathways of isoprenoid biosynthesis in *Arabidopsis thaliana*. *Proc. Natl. Acad.*  
533 *Sci. U. S. A.*, 6866-6871.

- Liao, P., Chen, X., Wang, M., Bach, T.J. and Chye, M.L. (2018) Improved fruit alpha-tocopherol, carotenoid, squalene and phytosterol contents through manipulation of Brassica juncea 3-HYDROXY-3-METHYLGLUTARYL-COA SYNTHASE1 in transgenic tomato. *Plant Biotechnol J* **16**, 784-796.
- Liao, P., Hemmerlin, A., Bach, T.J. and Chye, M.L. (2016) The potential of the mevalonate pathway for enhanced isoprenoid production. *Biotechnol Adv* **34**, 697-713.
- Liao, Z.H., Chen, M., Gong, Y. F., Miao, Z. Q., Sun, X. F., & Tang, K. X. (2006) Isoprenoid biosynthesis in plants: pathways, genes, regulation and metabolic engineering. *J Biol Sci* **6**, 209–219.
- Lu, X.M., Hu, X.J., Zhao, Y.Z., Song, W.B., Zhang, M., Chen, Z.L., Chen, W., Dong, Y.B., Wang, Z.H. and Lai, J.S. (2012) Map-based cloning of zb7 encoding an IPP and DMAPP synthase in the MEP pathway of maize. *Mol Plant* **5**, 1100-1112.
- Ma, D., Li, G., Zhu, Y. and Xie, D.Y. (2017) Overexpression and Suppression of Artemisia annua 4-Hydroxy-3-Methylbut-2-enyl Diphosphate Reductase 1 Gene (AaHDR1) Differentially Regulate Artemisinin and Terpenoid Biosynthesis. *Front Plant Sci* **8**, 77.
- Ma, Y., Yuan, L., Wu, B., Li, X., Chen, S. and Lu, S. (2012) Genome-wide identification and characterization of novel genes involved in terpenoid biosynthesis in Salvia miltiorrhiza. *J Exp Bot* **63**, 2809-2823.
- Mahmoud, S.S. and Croteau, R.B. (2001) Metabolic engineering of essential oil yield and composition in mint by altering expression of deoxyxylulose phosphate reductoisomerase and menthofuran synthase. *Proc Natl Acad Sci U S A* **98**, 8915-8920.
- Merret, R., Cirioni, J., Bach, T.J. and Hemmerlin, A. (2007) A serine involved in actin-dependent subcellular localization of a stress-induced tobacco BY-2 hydroxymethylglutaryl-CoA reductase isoform. *FEBS Lett* **581**, 5295-5299.
- Movahedi, A., Zhang, J., Amirian, R. and Zhuge, Q. (2014) An efficient Agrobacterium-mediated transformation system for poplar. *Int J Mol Sci* **15**, 10780-10793.
- Movahedi, A., Zhang, J., Sun, W., Mohammadi, K., Almasi Zadeh Yaghuti, A., Wei, H., Wu, X., Yin, T. and Zhuge, Q. (2018) Functional analyses of PtRDM1 gene overexpression in poplars and evaluation of its effect on DNA methylation and response to salt stress. *Plant Physiol Biochem* **127**, 64-73.
- Movahedi, A., Zhang, J.X., Yin, T.M. and Qiang, Z.G. (2015) Functional Analysis of Two Orthologous NAC Genes, CarNAC3, and CarNAC6 from Cicer arietinum, Involved in Abiotic Stresses in Poplar. *Plant Molecular Biology Reporter* **33**, 1539-1551.
- Munoz-Bertomeu, J., Sales, E., Ros, R., Arrillaga, I. and Segura, J. (2007) Up-regulation of an N-terminal truncated 3-hydroxy-3-methylglutaryl CoA reductase enhances production of essential oils and sterols in transgenic Lavandula latifolia. *Plant Biotechnol J* **5**, 746-758.
- Opitz, S., Nes, W.D. and Gershenzon, J. (2014) Both methylerythritol phosphate and mevalonate pathways contribute to biosynthesis of each of the major isoprenoid classes in young cotton seedlings. *Phytochemistry* **98**, 110-119.
- Perreca, E., Rohwer, J., Gonzalez-Cabanelas, D., Loreto, F., Schmidt, A., Gershenzon, J. and Wright, L.P. (2020) Effect of Drought on the Methylerythritol 4-Phosphate (MEP) Pathway in the Isoprene Emitting Conifer Picea glauca. *Front Plant Sci* **11**, 546295.
- Rahman, L., Kouno, H., Hashiguchi, Y., Yamamoto, H., Narbad, A., Parr, A., Walton, N., Ikenaga, T. and Kitamura, Y. (2009) HCHL expression in hairy roots of Beta vulgaris yields a high accumulation of p-hydroxybenzoic acid (pHBA) glucose ester, and linkage of pHBA into cell walls. *Bioresour Technol* **100**, 4836-4842.
- Ren, D., Liu, Y., Yang, K.Y., Han, L., Mao, G., Glazebrook, J. and Zhang, S. (2008) A fungal-responsive MAPK cascade regulates phytoalexin biosynthesis in Arabidopsis. *Proc Natl Acad Sci U S A* **105**, 5638-5643.
- Roberts, S.C. (2007) Production and engineering of terpenoids in plant cell culture. *Nat Chem Biol* **3**, 387-395.
- Rui, X., Caiqin, L., Wangjin, L., Juan, D., Zehuai, W. and Jianguo, L. (2012) 3-Hydroxy-3-methylglutaryl coenzyme A reductase 1 (HMG1) is highly associated with the cell division during the early stage of fruit

development which determines the final fruit size in Litchi chinensis. *Gene* **498**, 28-35.

Sakakibara, H. (2006) Cytokinins: activity, biosynthesis, and translocation. *Annu Rev Plant Biol* **57**, 431-449.

Schaller, H., Grausem, B., Benveniste, P., Chye, M.L., Tan, C.T., Song, Y.H. and Chua, N.H. (1995) Expression of the Hevea brasiliensis (H.B.K.) Mull. Arg. 3-Hydroxy-3-Methylglutaryl-Coenzyme A Reductase 1 in Tobacco Results in Sterol Overproduction. *Plant Physiol* **109**, 761-770.

Simpson, K., Quiroz, L.F., Rodriguez-Concepcion, M. and Stange, C.R. (2016) Differential Contribution of the First Two Enzymes of the MEP Pathway to the Supply of Metabolic Precursors for Carotenoid and Chlorophyll Biosynthesis in Carrot (Daucus carota). *Front Plant Sci* **7**, 1344.

Song, X., Yu, X., Hori, C., Demura, T., Ohtani, M. and Zhuge, Q. (2016) Heterologous Overexpression of Poplar SnRK2 Genes Enhanced Salt Stress Tolerance in Arabidopsis thaliana. *Front Plant Sci* **7**, 612.

Takahashi, S., Kuzuyama, T., Watanabe, H. and Seto, H. (1998) A 1-deoxy-D-xylulose 5-phosphate reductoisomerase catalyzing the formation of 2-C-methyl-D-erythritol 4-phosphate in an alternative nonmevalonate pathway for terpenoid biosynthesis. *Proc Natl Acad Sci U S A* **95**, 9879-9884.

Tiski, I., Marraccini, P., Pot, D., Vieira, L.G. and Pereira, L.F. (2011) Characterization and expression of two cDNA encoding 3-Hydroxy-3-methylglutaryl coenzyme A reductase isoforms in coffee (Coffea arabica L.). *OMICS* **15**, 719-727.

Vaccaro, M., Malafronte, N., Alfieri, M., De Tommasi, N. and Leone, A. (2014) Enhanced biosynthesis of bioactive abietane diterpenes by overexpressing AtDXS or AtDXR genes in Salvia sclarea hairy roots. *Plant Cell Tissue and Organ Culture* **119**, 65-77.

van Schie, C.C., Haring, M.A. and Schuurink, R.C. (2006) Regulation of terpenoid and benzenoid production in flowers. *Curr Opin Plant Biol* **9**, 203-208.

Wang, H., Nagegowda, D.A., Rawat, R., Bouvier-Nave, P., Guo, D., Bach, T.J. and Chye, M.L. (2012) Overexpression of Brassica juncea wild-type and mutant HMG-CoA synthase 1 in Arabidopsis up-regulates genes in sterol biosynthesis and enhances sterol production and stress tolerance. *Plant Biotechnol J* **10**, 31-42.

Wei, Y., Mohsin, A., Hong, Q., Guo, M. and Fang, H. (2018) Enhanced production of biosynthesized lycopene via heterogenous MVA pathway based on chromosomal multiple position integration strategy plus plasmid systems in Escherichia coli. *Bioresour Technol* **250**, 382-389.

Wille, A., Zimmermann, P., Vranova, E., Furlholz, A., Laule, O., Bleuler, S., Hennig, L., Prelic, A., von Rohr, P., Thiele, L., Zitzler, E., Gruissem, W. and Buhmann, P. (2004) Sparse graphical Gaussian modeling of the isoprenoid gene network in Arabidopsis thaliana. *Genome Biol* **5**, R92.

Xie, Z., Kapteyn, J. and Gang, D.R. (2008) A systems biology investigation of the MEP/terpenoid and shikimate/phenylpropanoid pathways points to multiple levels of metabolic control in sweet basil glandular trichomes. *Plant J* **54**, 349-361.

Xing, L., Zhang, D., Zhao, C., Li, Y., Ma, J., An, N. and Han, M. (2016) Shoot bending promotes flower bud formation by miRNA-mediated regulation in apple (Malus domestica Borkh.). *Plant Biotechnol J* **14**, 749-770.

Xing, S., Miao, J., Li, S., Qin, G., Tang, S., Li, H., Gu, H. and Qu, L.J. (2010) Disruption of the 1-deoxy-D-xylulose-5-phosphate reductoisomerase (DXR) gene results in albino, dwarf and defects in trichome initiation and stomata closure in Arabidopsis. *Cell Res* **20**, 688-700.

Xu, C., Wei, H., Movahedi, A., Sun, W., Ma, X., Li, D., Yin, T. and Zhuge, Q. (2019) Evaluation, characterization, expression profiling, and functional analysis of DXS and DXR genes of Populus trichocarpa. *Plant Physiol Biochem* **142**, 94-105.

Xu, J.W., Xu, Y.N. and Zhong, J.J. (2012) Enhancement of ganoderic acid accumulation by overexpression of an N-terminally truncated 3-hydroxy-3-methylglutaryl coenzyme A reductase gene in the basidiomycete Ganoderma lucidum. *Appl Environ Microbiol* **78**, 7968-7976.

Yamaguchi, S., Kamiya, Y., & Nambara, E. (2018) Regulation of ABA and GA levels during seed development

628 and germination in Arabidopsis. *Annu Plant Rev* **27**, 224–247.

629 Yang, J., Guo, L. (2014) Biosynthesis of  $\beta$ -carotene in engineered *E. coli* using the MEP and MVA pathways.

630 *Microb Cell Fact*, 160.

631 Zhang, H., Niu, D., Wang, J., Zhang, S., Yang, Y., Jia, H. and Cui, H. (2015) Engineering a Platform for

632 Photosynthetic Pigment, Hormone and Membrane-Related Diterpenoid Production in *Nicotiana tabacum*.

633 *Plant Cell Physiol* **56**, 2125-2138.

634 Zhang, J., Li, J., Liu, B., Zhang, L., Chen, J. and Lu, M. (2013) Genome-wide analysis of the *Populus* Hsp90 gene

635 family reveals differential expression patterns, localization, and heat stress responses. *BMC Genomics*

636 **14**, 532.

637 Zhang, K.K., Fan, W., Huang, Z.W., Chen, D.F., Yao, Z.W., Li, Y.F., Yang, Y.F. and Qiu, D.Y. (2019) Transcriptome

638 analysis identifies novel responses and potential regulatory genes involved in 12-deoxyphorbol-13-

639 phenylacetate biosynthesis of *Euphorbia resinifera*. *Industrial Crops and Products* **135**, 138-145.

640 Zhang, L., Ding, R., Chai, Y., Bonfill, M., Moyano, E., Oksman-Caldentey, K.M., Xu, T., Pi, Y., Wang, Z., Zhang,

641 H., Kai, G., Liao, Z., Sun, X. and Tang, K. (2004) Engineering tropane biosynthetic pathway in

642 *Hyoscyamus niger* hairy root cultures. *Proc Natl Acad Sci U S A* **101**, 6786-6791.

643 Zhang, Y., Zhao, Y., Wang, J., Hu, T., Tong, Y., Zhou, J., Song, Y., Gao, W. and Huang, L. (2018) Overexpression

644 and RNA interference of TwDXR regulate the accumulation of terpenoid active ingredients in

645 *Tripterygium wilfordii*. *Biotechnol Lett* **40**, 419-425.

646

## 647 6. Figure legends

648 **Figure 1 | MEP- and MVA-related genes analyses in overexpressed *PtHMGR*- and *PtDXR*-O**

649 ***Es poplars*. a**, MVA-related genes *AACT*, *HMGS*, *MVK*, *MVD*, and *FPS* affected by *PtHMGR* over

650 expressing. **b**, MEP-related genes *DXS*, *MCT*, *CMK*, *HDS*, *HDR*, *IDI*, *GPS*, *GPPS*, and *DXR* affected

651 by *PtHMGR* overexpressing. **c**, MVA-related genes *AACT*, *HMGS*, *HMGR*, *MVK*, *MVD*, and *FP*

652 *S* affected by *PtDXR* overexpressing. **d**, MEP-related genes *DXS*, *DXR*, *MCT*, *CMK*, *HDS*, *HDR*, *ID*

653 *I*, *GPS*, and *GPPS* affected by *PtDXR* overexpressing. *PtActin* was used as an internal reference

654 in all repeats; \*  $P < 0.05$ , \*\*  $P < 0.01$ , \*\*\*  $P < 0.001$ , \*\*\*\*  $P < 0.0001$ ; Three independent repli

655 cations were performed in this experiment.

656 **Figure 2 | HPLC-MS/MS content analyses of lycopene,  $\beta$ -carotene, Lutein, and real-time PCR**

657 **of *ZEP* and *NCED* genes family**. HPLC-MS/MS content analyses have been performed to show

658 the effect of *PtHMGR*-OEs on **a**, lycopene **b**,  $\beta$ -carotene, and **c**, lutein. Relative expressions

659 have been analyzed affected by *PtHMGR*-OEs comparing with NT poplars of **d**, *ZEP*,

660 and **e**, *NCED* genes family. Bars represent mean  $\pm$  SD ( $n = 3$ ); Stars reveal significant differences,

661 \*  $P < 0.05$ , \*\*  $P < 0.01$ , \*\*\*  $P < 0.001$ , \*\*\*\*  $P < 0.0001$ ; Three independent experiments were

662 performed in these analyses.

663 **Figure 3 | HPLC-MS/MS content analyses of lycopene,  $\beta$ -carotene, Lutein, and real-time PCR**

664 **of *ZEP* and *NCED* genes family**. HPLC-MS/MS content analyses have been performed to show



the effect of *PtDXR*-OEs on **a**, lycopene **b**,  $\beta$ -carotene, and **c**, lutein. Relative expressions have been analyzed affected by *PtDXR*-OEs comparing with NT poplars of **d**, *ZEP*, and **e**, *NCED* genes family. Bars represent mean  $\pm$  SD (n = 3); Stars reveal significant differences, \* P < 0.05, \*\* P < 0.01, \*\*\* P < 0.001, \*\*\*\*P < 0.0001; Three independent experiments were performed in these analyses.

**Figure 4 | HPLC-MS/MS content analyses of MEP- and MVA-derived isoprenoids. a,b,c,d, and e**, Violin plots reveal the contents of isoprenoids GA3, tZR, IPA, DCS, and CS obtained from MEP- and MVA-pathways influenced by *PtHMGR*- and *PtDXR*-OEs. **f,g,h,i, and j**, the column plots reveal the effect of *PtHMGR*-OE3 and -7 and *PtDXR*-OE1 and -3 on the mentioned above isoprenoids separately; NT poplars have been used as the control. Bars represent mean  $\pm$  SD (n = 3); Stars reveal significant differences, \*P < 0.05, \*\*P < 0.01, \*\*\*P < 0.001, \*\*\*\*P < 0.0001. k,l,m,n, and o, represent the HPLC-MS/MS chromatogram content analyses of GA3, tZR, IPA, DCS, and CS, respectively affected by *PtHMGR*- and *PtDXR*-OEs comparing with NT poplars.

**Figure 5 | Phenotypic changes resulted by affected MVA- and MEP- pathway interactions in 45-day-old poplars. a**, Mean comparisons of stem lengths revealed significantly higher lengths *PtDXR*-OEs than NT poplars compared with *PtHMGR*-OEs. *PtHMGR* transgenics also revealed significantly higher lengths than NT poplars. **b**, Mean comparisons of *ZEP* and *NCED* relative expressions between *PtHMGR*- and *PtDXR*-OEs compared to NT poplars. **c**, Mean comparisons of stem diameters revealed less significant differences between *PtDXR*-OEs and NT poplars. Stars reveal significant differences, \*P < 0.05, \*\*P < 0.01, \*\*\*P < 0.001, \*\*\*\*P < 0.0001. **d(I)**, The *PtDXR* transgenic revealed a higher stem length than *PtHMGR*-OEs and NT poplars. **d(II)**, The *PtHMGR* transgenic presents an insignificantly more stem development than NT poplar. **d(III)**, NT poplar was used as a control; Scale bar represents 1 cm.

**Figure 6 | The interactions between MEP- and MVA-pathways.** The IPP and DMAPP are considered the common precursors of the MEP- and MVA-pathways between cytoplasm and plastid. In addition, the putative communication generates between MVA- and MEP-related genes and MVA- and MEP-derived products. MVA: mevalonic acid, MEP: methylerythritol phosphate, IPP: isopentenyl diphosphate, DMAPP: dimethylallyl diphosphate, AACT: acetoacetyl CoA thiolase, HMGS: 3-hydroxy-3-methylglutaryl-CoA synthase, HMG-CoA: 3-hydroxy-3-methylglutaryl-CoA, HMGR: 3-hydroxy-3-methylglutaryl-CoA reductase, MVK:

mevalonate kinase, MVD: mevalonate5-diphosphate decarboxylase, IPP: isopentenyl diphosphate, IDI: IPP isomerase, GPP: geranyldiphosphate, FPP: farnesyl diphosphate, GPS: geranyl phosphate synthase, FPS: farnesyl-diphosphate synthase, GPPS: geranyl diphosphate synthase, GGPPS: geranyl geranyl diphosphate synthase, DXS: 1-deoxy-D-xylulose5-phosphate synthase, DXP: 1-deoxy-D-xylulose5-phosphate, DXR: 1-deoxy-D-xylulose5-phosphate reductoisomerase, HDS: 1-hydroxy-2-methyl-2-(E)-butenyl4-diphosphate synthase, HDR: 1-hydroxy-2-methyl-2-(E)-butenyl4-diphosphate reductase, MCT: MEP cytidyltransferase, CMK: 4-diphosphocytidyl-2-C-methyl-D-erythritol kinase.

#### Supplemental figures and table

**Supplemental Figure 1 | Amino acid sequences alignment of PtHMGR protein and other known HMGR proteins.** *A. thaliana* (NP\_177775.2), *G. hirsutum* (XP\_016691783.1), *M. domestica* (XP\_008348952.1), *M. esculenta* (XP\_021608133.1), *P. persica* (XM\_020569919.1), *O. sativa* (XM\_015768351.2), *T. cacao* (XM\_007043046.2), *Z. mays* (PWZ28886.1). The HMG-CoA and NADPH binding domains are indicated in red rectangular.

**Supplemental Figure 2 | Construction of a phylogenetic tree based on the HMGR sequences of various species.** Accession numbers of the HMGR obtained from Phytozome are as follows: *A. thaliana* (AT1G76490 and AT2G17370), *P. trichocarpa* (Potri.011G145000, Potri.005G257000, Potri.004G208500, Potri.001G457000, Potri.009G169900 and Potri.002G004000), *Gossypium raimondii* (Gorai.008G013000, Gorai.002G146000, Gorai.002G014700, Gorai.005G215800, Gorai.012G138100, Gorai.005G215500, Gorai.005G215600 and Gorai.005G215700), *Malus domestica* (MDP0000157996, MDP0000268909, MDP0000372490, MDP0000251253 and MDP0000312032), *Manihot esculenta* (Manes.15G114100, Manes.01G157500, Manes.03G096600, Manes.02G116900 and Manes.05G128600), *Oryza sativa* (LOC\_Os09g31970, LOC\_Os08g40180 and LOC\_Os02g48330), *Prunus persica* (Prupe.7G187000, Prupe.7G187500 and Prupe.8G182300), *Theobroma cacao* (Thecc1EG000025, Thecc1EG007601 and Thecc1EG034814), and *Zea mays* (GRMZM2G393337, GRMZM2G058095, GRMZM2G136465, GRMZM2G001645 and GRMZM2G043503).

**Supplemental Figure 3 | Molecular identification of PtHMGR-OEs.** (A) PCR identification of PtHMGR in PtHMGR-OEs and NT poplars. Lane M: 15K molecular mass marker (TransGen, China); lane 1: genome DNA from WT as negative control; lanes 2–9: genome DNA from



*PtHMGR-OE* lines (B) qRT-PCR identification of the transcript levels of *PtHMGR* in *PtHMGR-OEs* and NT poplars. Three independent experiments were performed; Stars reveal significant differences, \*  $P < 0.05$ , \*\*  $P < 0.01$ , \*\*\*  $P < 0.001$ .

**Supplemental Figure 4** | HPLC chromatograms of analyzing the contents of (A)  $\beta$ -carotene, (B) lycopene, and (C) lutein in NT poplars and *PtHMGR-OEs*.

**Supplemental Figure 5** | HPLC-MS/MS chromatogram analyses of the contents of (A) GA3, (B) TZR, (C) IPA, (D) DCS, and (E) CS affected by *PtHMGR-OE3* and -7 comparing with NT poplars.

**Supplemental Figure 6** | Chromatogram analyses of GA3 standards via HPLC-MS/MS. The chromatogram of standard GA3 at (A) 0.1, (B) 0.2, (C) 0.5, (D) 2, (E) 5, (F) 20, (G) 50, and (H) 200 ng/mL concentrations. (I) Equations for the GA3 standard curves.

**Supplemental Figure 7** | Chromatogram analyses of tZR standards via HPLC-MS/MS. The chromatogram of standard tZR at (A) 0.1, (B) 0.2, (C) 0.5, (D) 2, (E) 5, (F) 20, (G) 50, and (H) 200 ng/mL concentrations. (I) Equations for the tZR standard curves.

**Supplemental Figure 8** | Chromatogram analyses of IPA standards via HPLC-MS/MS. The chromatogram of standard IPA at (A) 0.2, (B) 0.5, (C) 2, (D) 5, (E) 20, (F) 50, and (G) 200 ng/mL concentrations. (H) Equations for the IPA standard curves.

**Supplemental Figure 9** | Chromatogram analyses of DCS standards via HPLC-MS/MS. The chromatogram of standard DCS at (A) 0.5, (B) 2, (C) 10, (D) 20, and (E) 50 ng/mL concentrations. (F) Equations for the DCS standard curves.

**Supplemental Figure 10** | Chromatogram analyses of CS standards via HPLC-MS/MS. The chromatogram of standard CS at (A) 0.5, (B) 5, (C) 10, (D) 20, and (E) 50 ng/mL concentrations. (F) Equations for the CS standard curves.

**Supplemental Table 1** | Primers were used in this study.

**Supplemental Table 2** | Table of data analyses used in phenotypic changes evaluation. **a**, Stem diameter data analyses. **b**, Stem length data analyses.

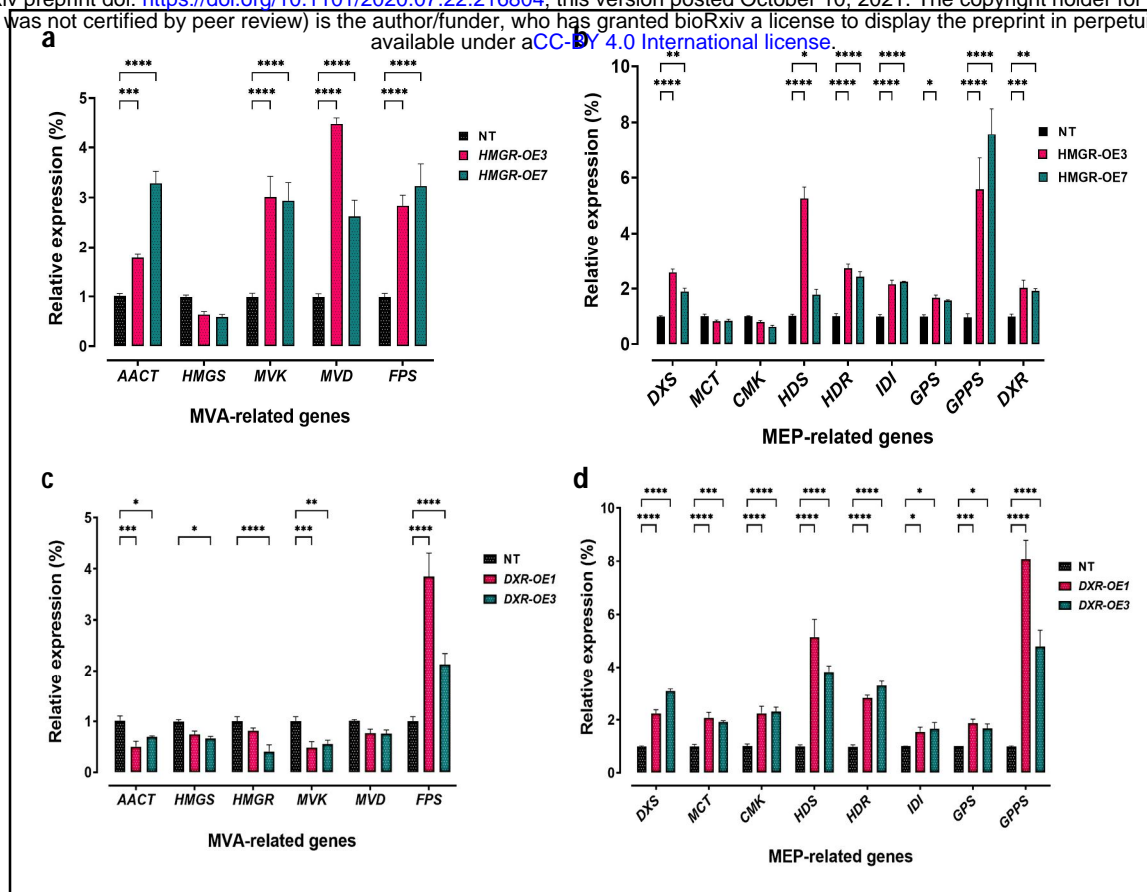


**Figure 1 | MEP- and MVA-related genes analyses in overexpressed *PtHMGR*- and *PtDXR*-OEs poplars.** **a**, MVA-related genes *AACT*, *HMGS*, *MVK*, *MVD*, and *FPS* affected by *PtHMGR* overexpressing. **b**, MEP-related genes *DXS*, *MCT*, *CMK*, *HDS*, *HDR*, *IDI*, *GPS*, *GPPS*, and *DXR* affected by *PtHMGR* overexpressing. **c**, MVA-related genes *AACT*, *HMGS*, *HMGR*, *MVK*, *MVD*, and *FPS* affected by *PtDXR* overexpressing. **d**, MEP-related genes *DXS*, *DXR*, *MCT*, *CMK*, *HDS*, *HDR*, *IDI*, *GPS*, and *GPPS* affected by *PtDXR* overexpressing. *PtActin* was used as an internal reference in all repeats; \*  $P < 0.05$ , \*\*  $P < 0.01$ , \*\*\*  $P < 0.001$ , \*\*\*\*  $P < 0.0001$ ; Three independent replications were performed in this experiment.

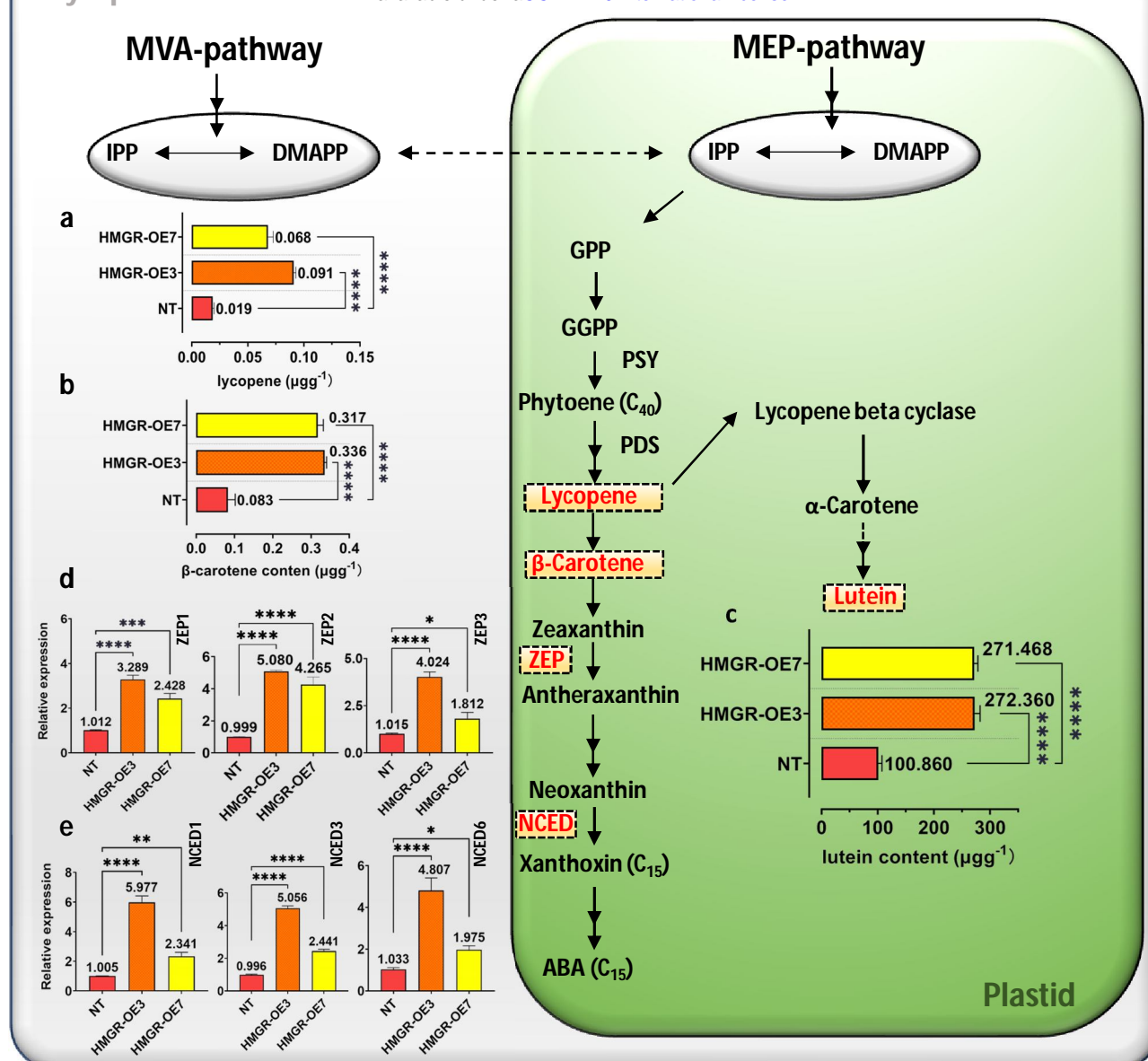


**Figure 2 | HPLC-MS/MS content analyses of lycopene,  $\beta$ -carotene, lutein, and real-time PCR of *ZEP* and *NCED* genes family.** HPLC-MS/MS content analyses have been performed to show the effect of *PtHMGR-OEs* on **a**, lycopene **b**,  $\beta$ -carotene, and **c**, lutein. Relative expressions have been analyzed affected by *PtHMGR-OEs* comparing with NT poplars of **d**, *ZEP*, and **e**, *NCED* genes family. Bars represent mean  $\pm$  SD (n = 3); Stars reveal significant differences, \* P < 0.05, \*\* P < 0.01, \*\*\* P < 0.001, \*\*\*\*P < 0.0001; Three independent experiments were performed in these analyses.

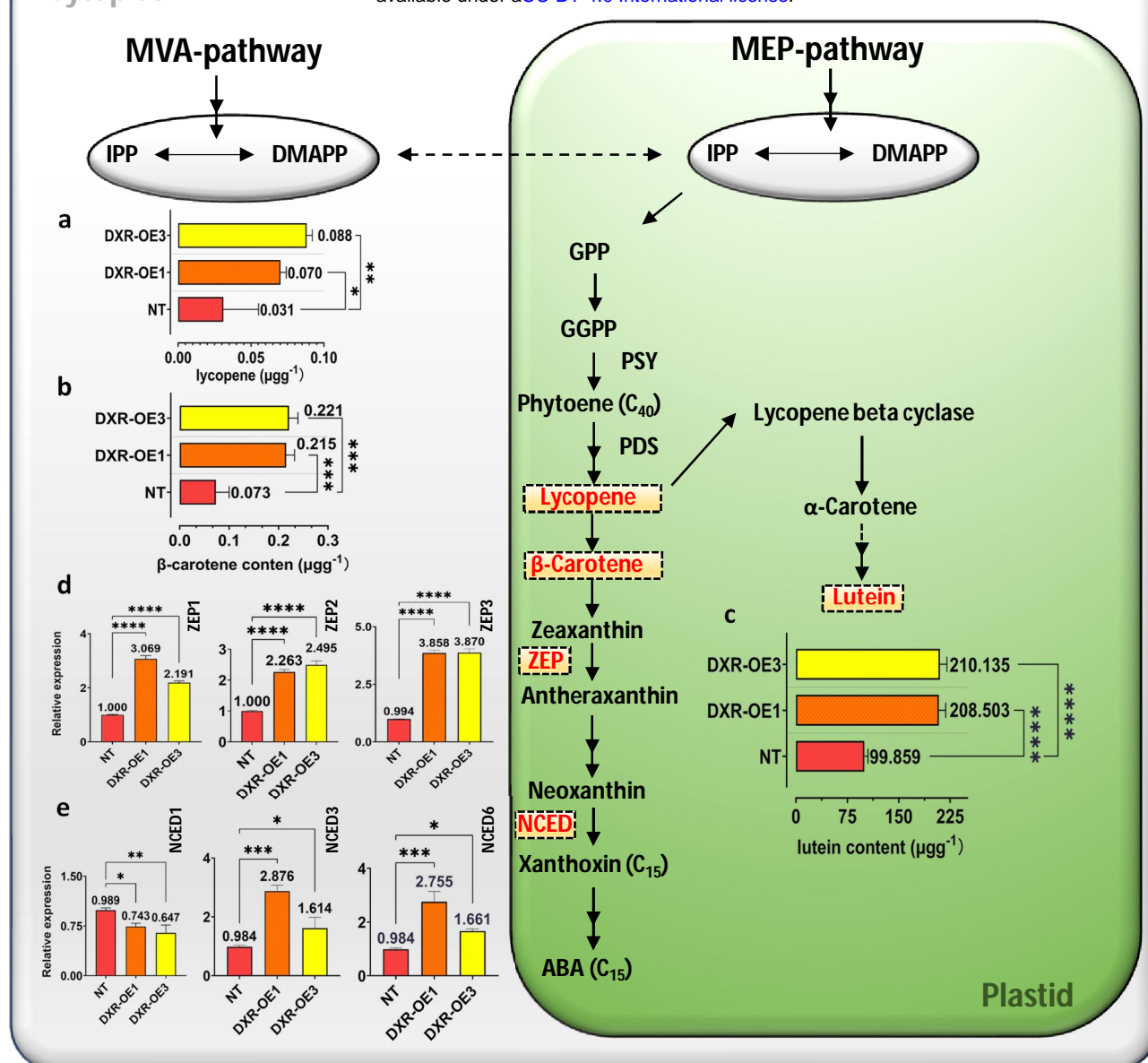


**Figure 3 | HPLC-MS/MS content analyses of lycopene,  $\beta$ -carotene, lutein, and real-time PCR of *ZEP* and *NCED* genes family.** HPLC-MS/MS content analyses have been performed to show the effect of *PtDXR-OEs* on **a**, lycopene **b**,  $\beta$ -carotene, and **c**, lutein. Relative expressions have been analyzed affected by *PtDXR-OEs* comparing with NT poplars of **d**, *ZEP*, and **e**, *NCED* genes family. Bars represent mean  $\pm$  SD (n = 3); Stars reveal significant differences, \*  $P < 0.05$ , \*\*  $P < 0.01$ , \*\*\*  $P < 0.001$ , \*\*\*\*  $P < 0.0001$ ; Three independent experiments were performed in these analyses.

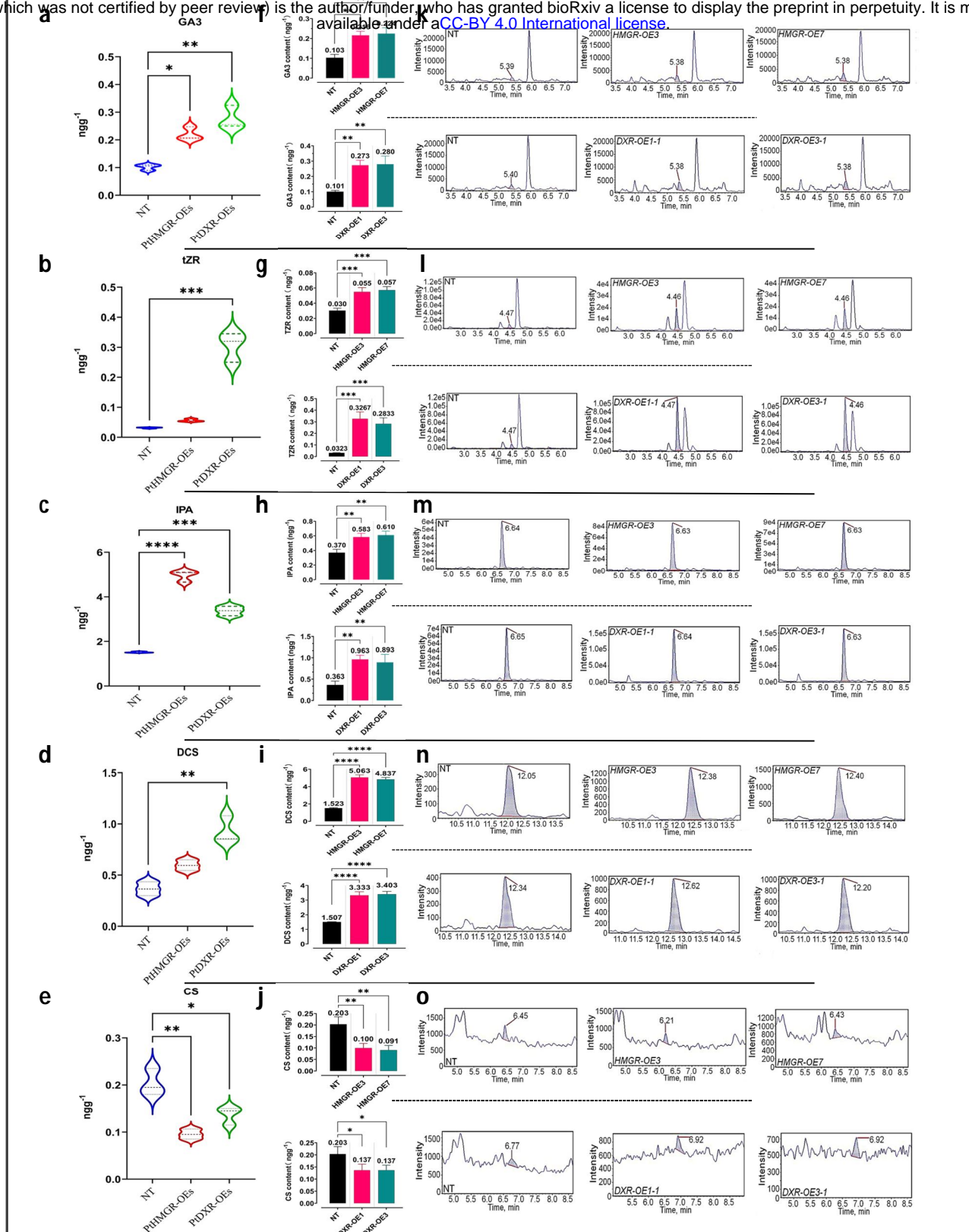


**Figure 4 | HPLC-MS/MS content analyses of MEP- and MVA-derived isoprenoids. a,b,c,d, and e,** Violin plots reveal the contents of isoprenoids GA3, tZR, IPA, DCS, and CS obtained from MEP- and MVA-pathways influenced by *PtHMGR*- and *PtDXR*-OEs. **f,g,h,i, and j,** the column plots reveal the effect of *PtHMGR*-OE3 and -7 and *PtDXR*-OE1 and -3 on the mentioned above isoprenoids separately; NT poplars have been used as the control. Bars represent mean  $\pm$  SD (n = 3); Stars reveal significant differences, \*P < 0.05, \*\*P < 0.01, \*\*\*P < 0.001, \*\*\*\*P < 0.0001. **k,l,m,n, and o,** represent the HPLC-MS/MS chromatogram content analyses of GA3, tZR, IPA, DCS, and CS, respectively affected by *PtHMGR*- and *PtDXR*-OEs comparing with NT poplars.



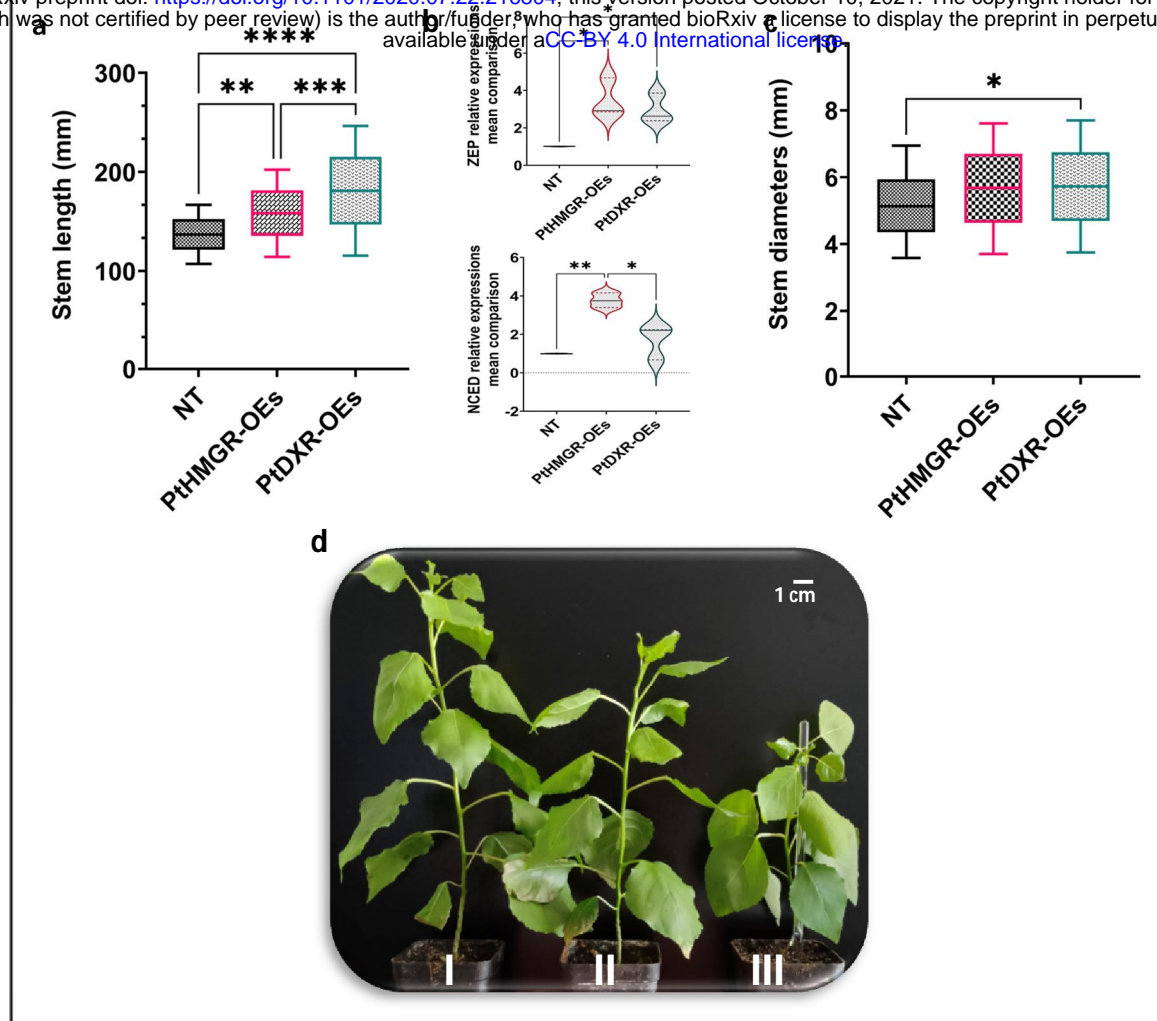


**Figure 5 | Phenotypic changes resulted by affected MVA- and MEP- pathway interactions in 45-day-old poplars.** **a**, Mean comparisons of stem lengths revealed significantly higher lengths *PtDXR-OEs* than NT poplars compared with *PtHMGR-OEs*. *PtHMGR* transgenics also revealed significantly higher lengths than NT poplars. **b**, Mean comparisons of *ZEP* and *NCED* relative expressions between *PtHMGR*- and *PtDXR-OEs* compared to NT poplars. **c**, Mean comparisons of stem diameters revealed less significant differences between *PtDXR-OEs* and NT poplars. Stars reveal significant differences, \* $P < 0.05$ , \*\* $P < 0.01$ , \*\*\* $P < 0.001$ , \*\*\*\* $P < 0.0001$ . **d**(I), The *PtDXR* transgenic revealed a higher stem length than *PtHMGR-OEs* and NT poplars. **d**(II), The *PtHMGR* transgenic presents an insignificantly more stem development than NT poplar. **d**(III), NT poplar was used as a control; Scale bar represents 1 cm.

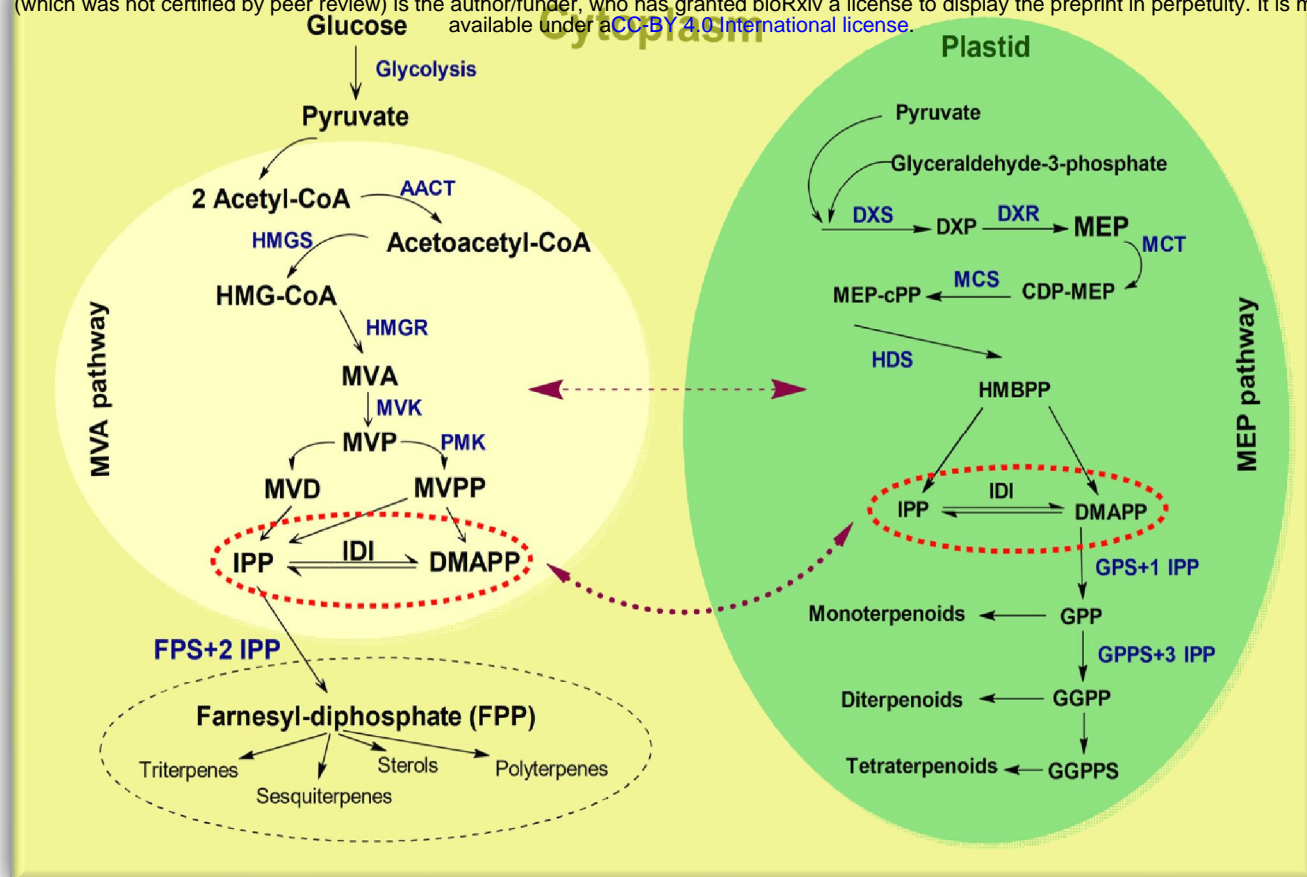
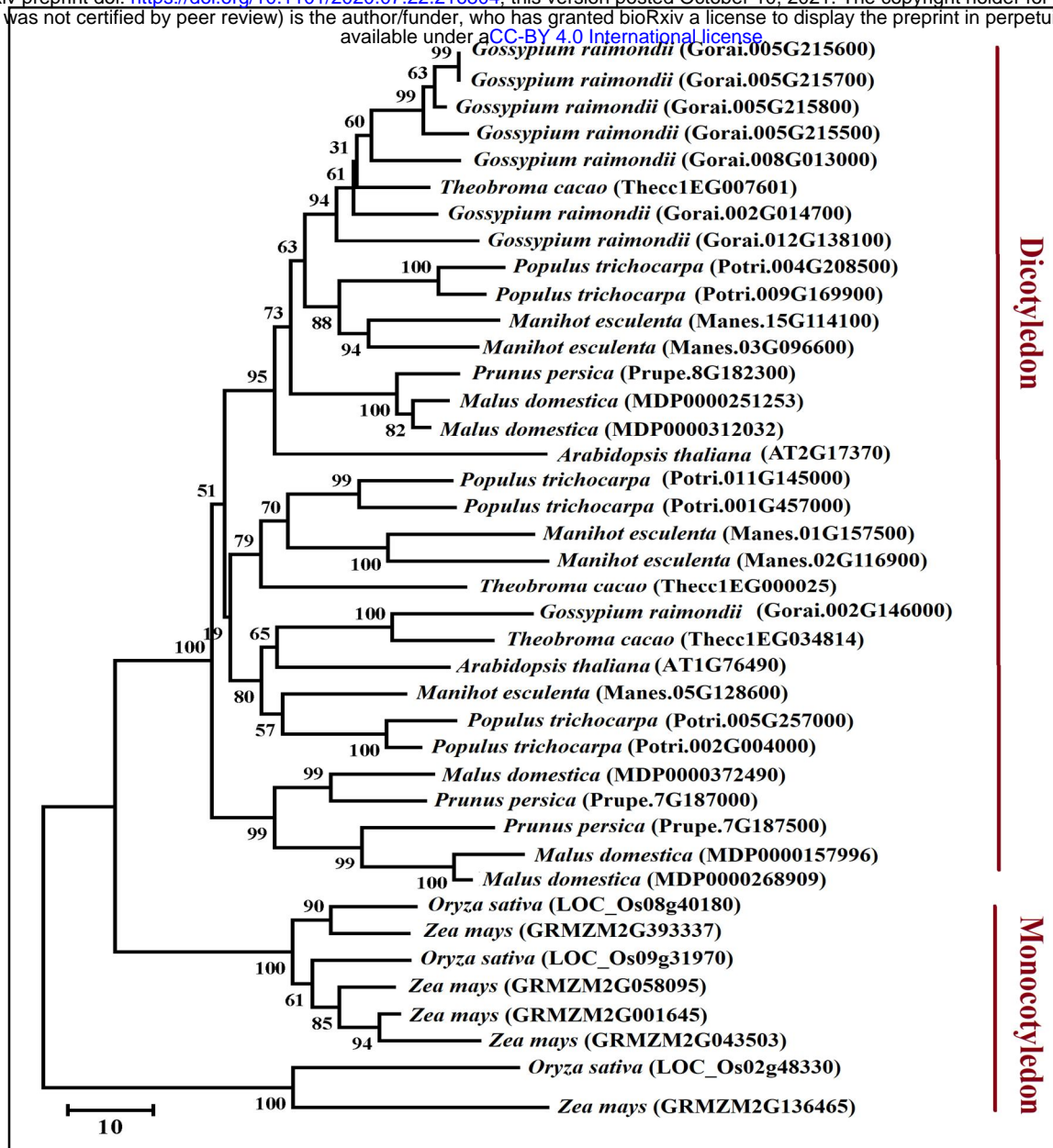


**Figure 6 | The interactions between MEP- and MVA-pathways.** The IPP and DMAPP are considered the common precursors of the MEP- and MVA-pathway between cytoplasm and plastid. In addition, the putative communication generates between MVA- and MEP-related genes and MVA- and MEP-derived products. MVA: mevalonic acid, MEP: methylerythritol phosphate, IPP: isopentenyl diphosphate, DMAPP: dimethylallyl diphosphate, AACT: acetoacetyl CoA thiolase, HMGS: 3-hydroxy-3-methylglutaryl-CoA synthase, HMG-CoA: 3-hydroxy-3-methylglutaryl-CoA, HMGR: 3-hydroxy-3-methylglutaryl-CoA reductase, MVK: mevalonate kinase, MVD: mevalonate5-diphosphate decarboxylase, IPP: isopentenyl diphosphate, IDI: IPP isomerase, GPP: geranyldiphosphate, FPP: farnesyl-diphosphate, GPS: geranyl phosphate synthase, FPS: farnesyl-diphosphate synthase, GPPS: geranyl diphosphate synthase, GGPPS: geranyl geranyl diphosphate synthase, DXS: 1-deoxy-D-xylulose5-phosphate synthase, DXP: 1-deoxy-D-xylulose5-phosphate, DXR: 1-deoxy-D-xylulose5-phosphate reductoisomerase, HDS: 1-hydroxy-2-methyl-2-(E)-butenyl4-diphosphate synthase, HDR: 1-hydroxy-2-methyl-2-(E)-butenyl4-diphosphate reductase, MCT: MEP cytidyltransferase, CMK: 4-diphosphocytidyl-2-C-methyl-D-erythritol kinase.

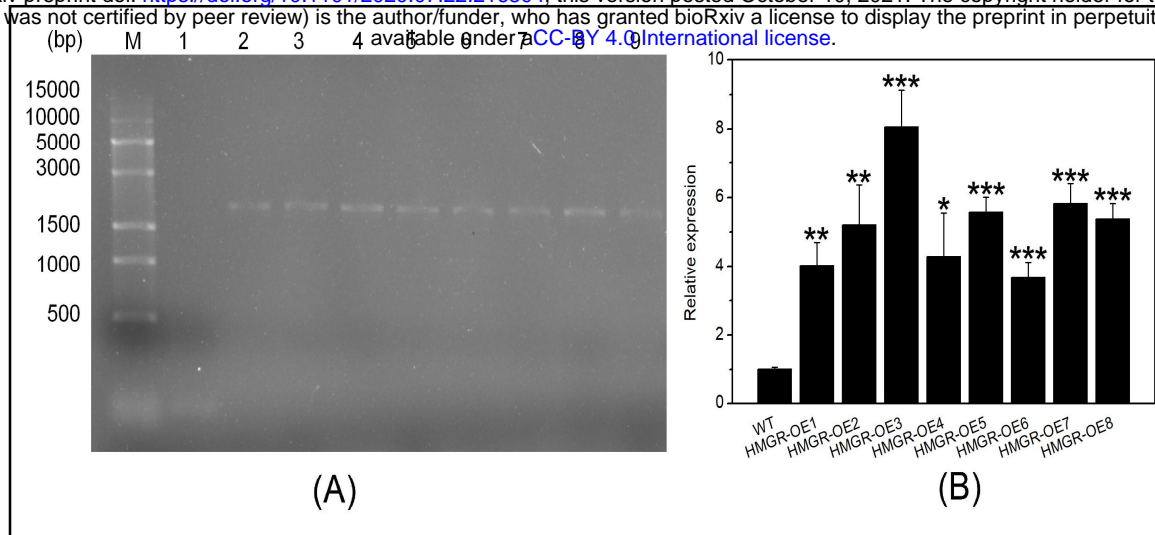




**Supplemental Figure 1 | Amino acid sequences alignment of PtHMGR protein and other known HMGR proteins.** *A. thaliana* (NP\_177775.2), *G. hirsutum* (XP\_016691783.1), *M. domestica* (XP\_008348952.1), *M. esculenta* (XP\_021608133.1), *P. persica* (XM\_020569919.1), *O. sativa* (XM\_015768351.2), *T. cacao* (XM\_007043046.2), *Z. mays* (PWZ28886.1). The HMG-CoA and NADPH binding domains are indicated in red rectangular.

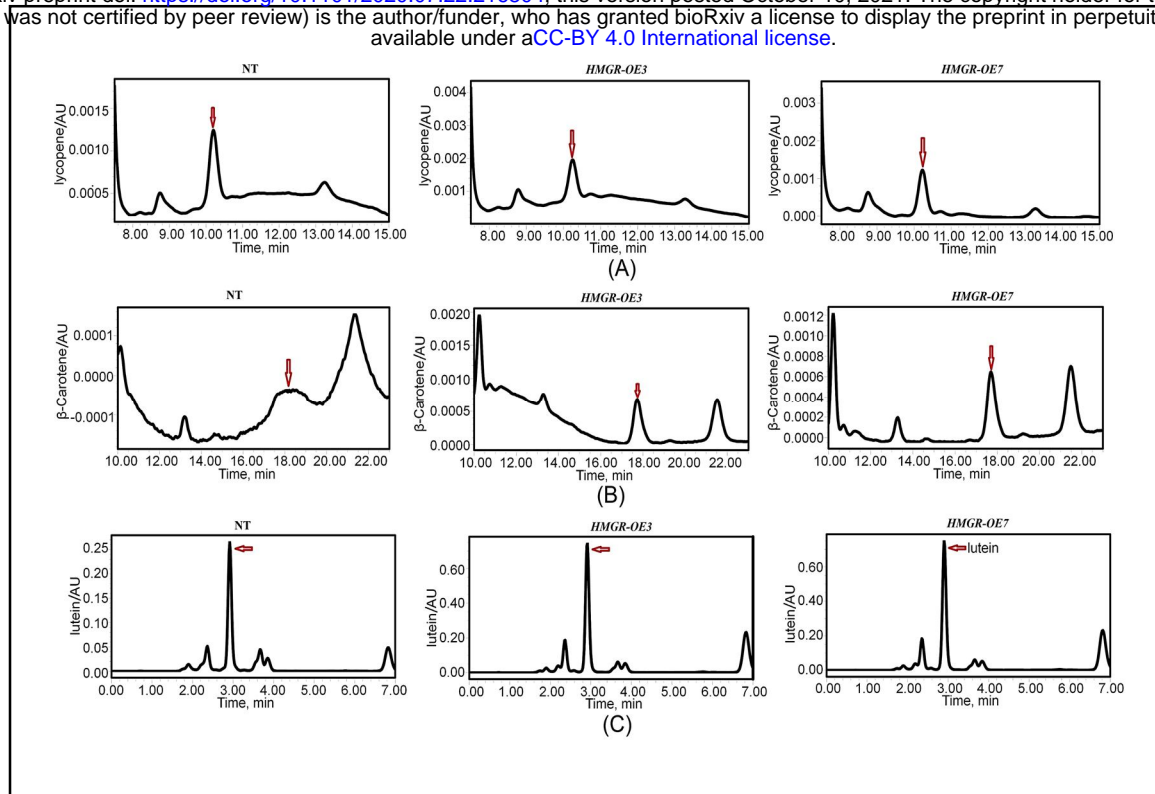


**Supplemental Figure 2 | Construction of a phylogenetic tree based on the *HMGR* sequences of various species.** Accession numbers of the *HMGR* obtained from Phytozome are as follows: *A. thaliana* (AT1G76490 and AT2G17370), *P. trichocarpa* (Potri.011G145000, Potri.005G257000, Potri.004G208500, Potri.001G457000, Potri.009G169900 and Potri.002G004000), *Gossypium raimondii* (Gorai.008G013000, Gorai.002G146000, Gorai.002G014700, Gorai.005G215800, Gorai.012G138100, Gorai.005G215500, Gorai.005G215600 and Gorai.005G215700), *Malus domestica* (MDP0000157996, MDP0000268909, MDP0000372490, MDP0000251253 and MDP0000312032), *Manihot esculenta* (Manes.15G114100, Manes.01G157500, Manes.03G096600, Manes.02G116900 and Manes.05G128600), *Oryza sativa* (LOC\_Os09g31970, LOC\_Os08g40180 and LOC\_Os02g48330), *Prunus persica* (Prupe.7G187000, Prupe.7G187500 and Prupe.8G182300), *Theobroma cacao* (Thecc1EG000025, Thecc1EG007601 and Thecc1EG034814), and *Zea mays* (GRMZM2G393337, GRMZM2G058095, GRMZM2G136465, GRMZM2G001645 and GRMZM2G043503).

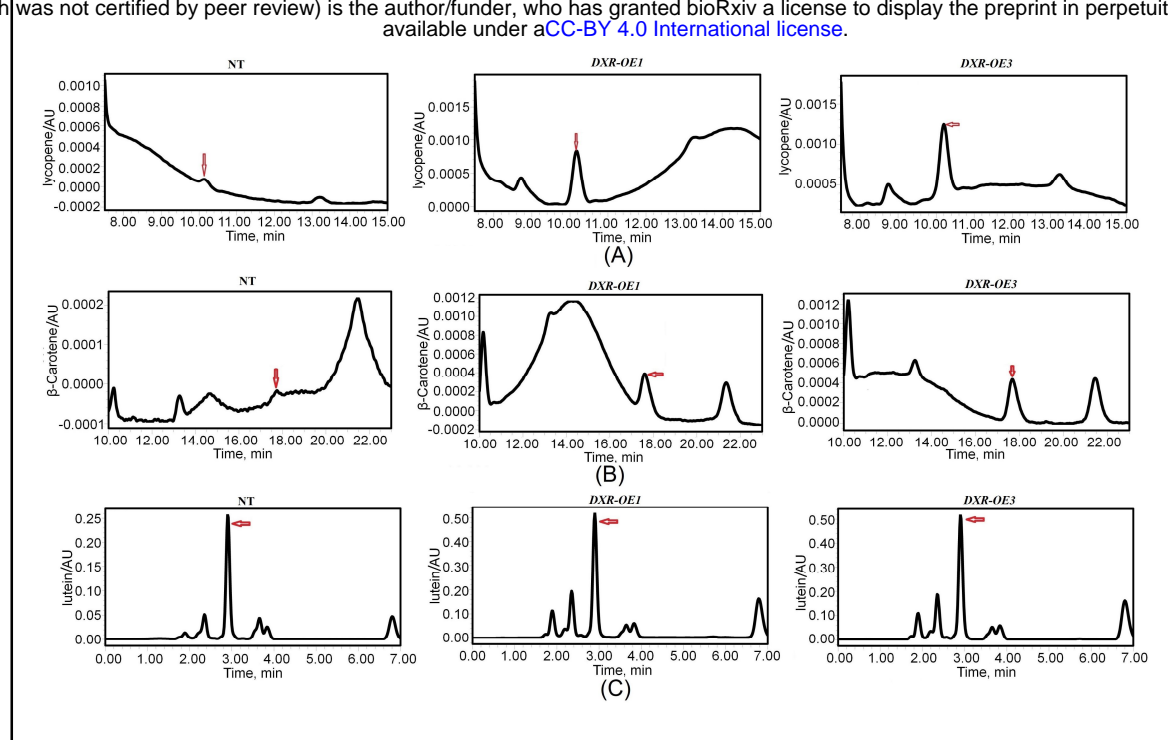


**Supplemental Figure 3 | Molecular identification of *PtHMGR-OEs*.** **(A)** PCR identification of *PtHMGR* in *PtHMGR-OEs* and NT poplars. Lane M: 15K molecular mass marker (TransGen, China); lane 1: genomic DNA from WT as a negative control; lanes 2–9: genomic DNAs from *PtHMGR-OE* lines. **(B)** qRT-PCR identification of the transcript levels of *PtHMGR* in *PtHMGR-OEs* and NT poplars. Three independent experiments were performed; Stars reveal significant differences, \* P < 0.05, \*\* P < 0.01, \*\*\* P < 0.001.

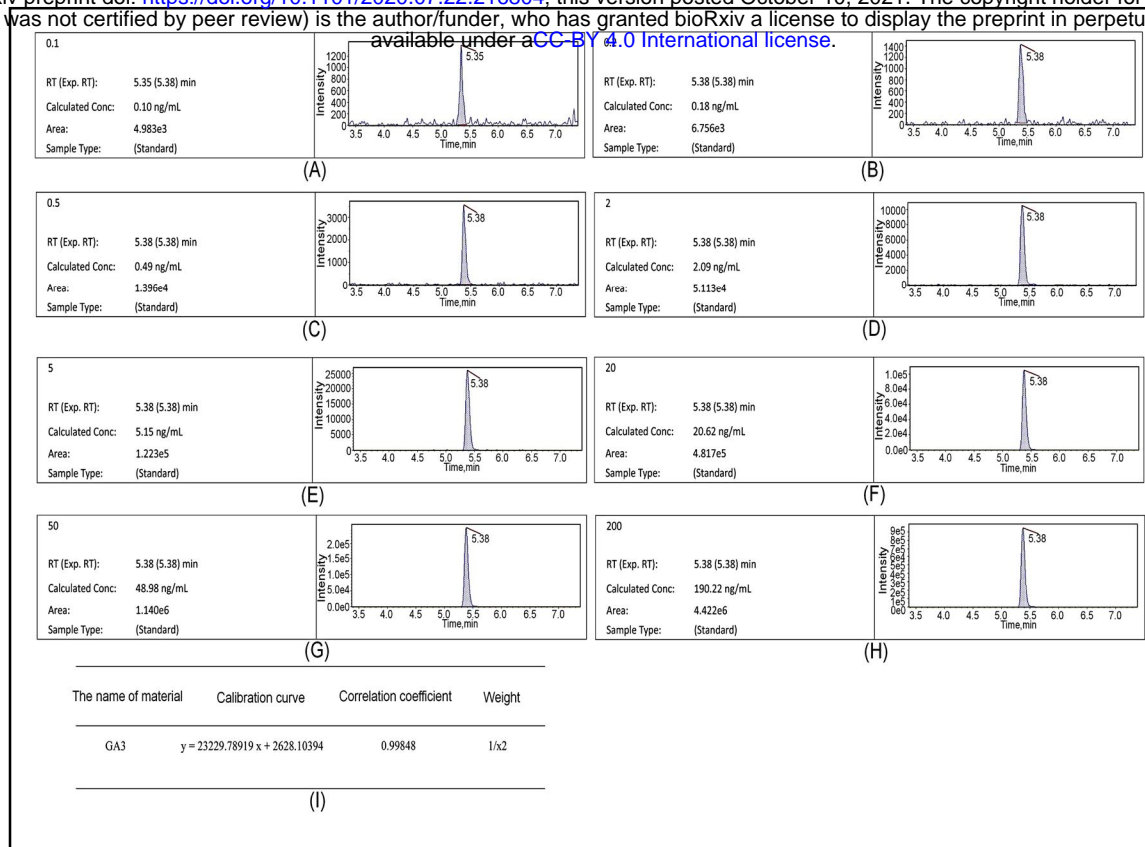




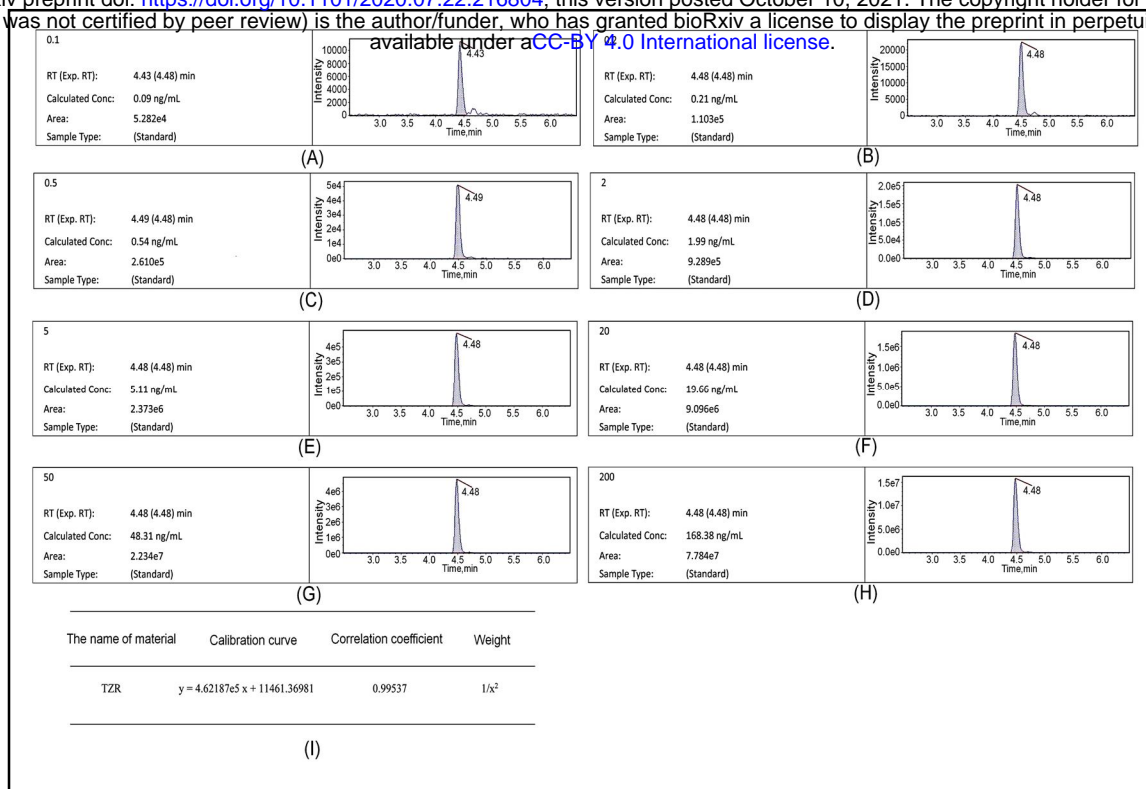
**Supplemental Figure 4** | HPLC chromatograms of analyzing the contents of (A)  $\beta$ -carotene, (B) lycopene, and (C) lutein in NT poplars and *PtHMGR-OEs*.



**Supplemental Figure 5 |** HPLC chromatograms of analyzing the contents of (A)  $\beta$ -carotene, (B) lycopene, and (C) lutein in NT poplars and *PtDXR-OEs*.

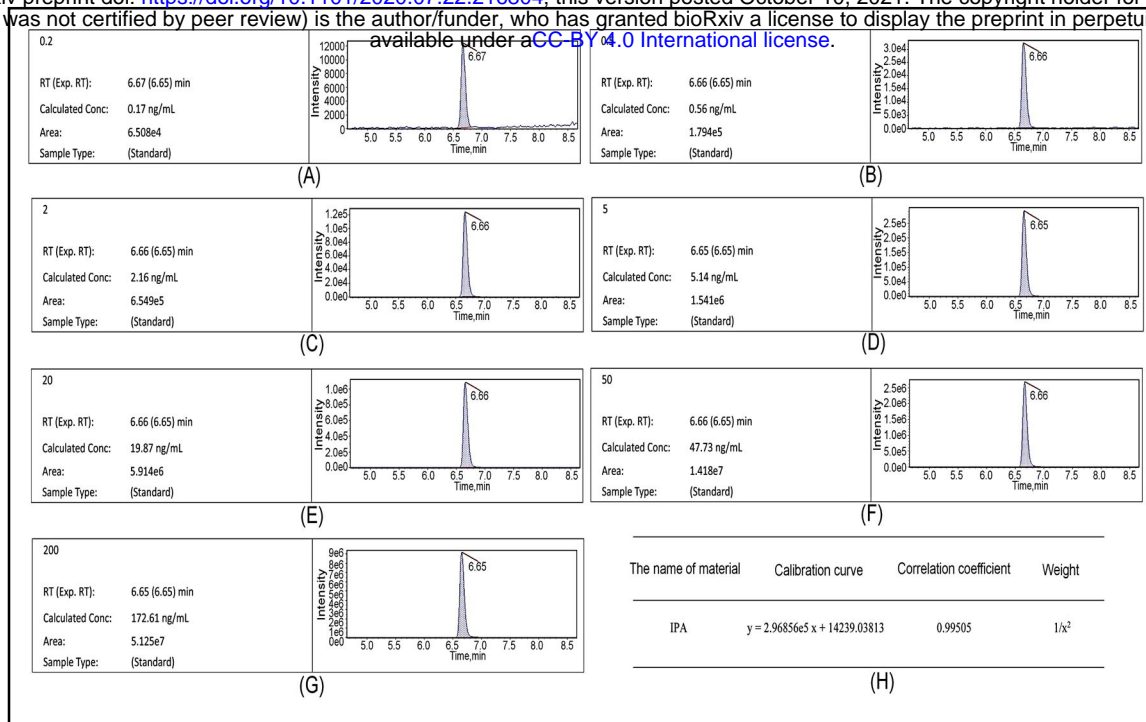


**Supplemental Figure 6 | Chromatogram analyses of GA3 standards via HPLC-MS/MS.** The chromatogram of standard GA3 at (A) 0.1, (B) 0.2, (C) 0.5, (D) 2, (E) 5, (F) 20, (G) 50, and (H) 200 ng/mL concentrations. (I) Equations for the GA3 standard curves.

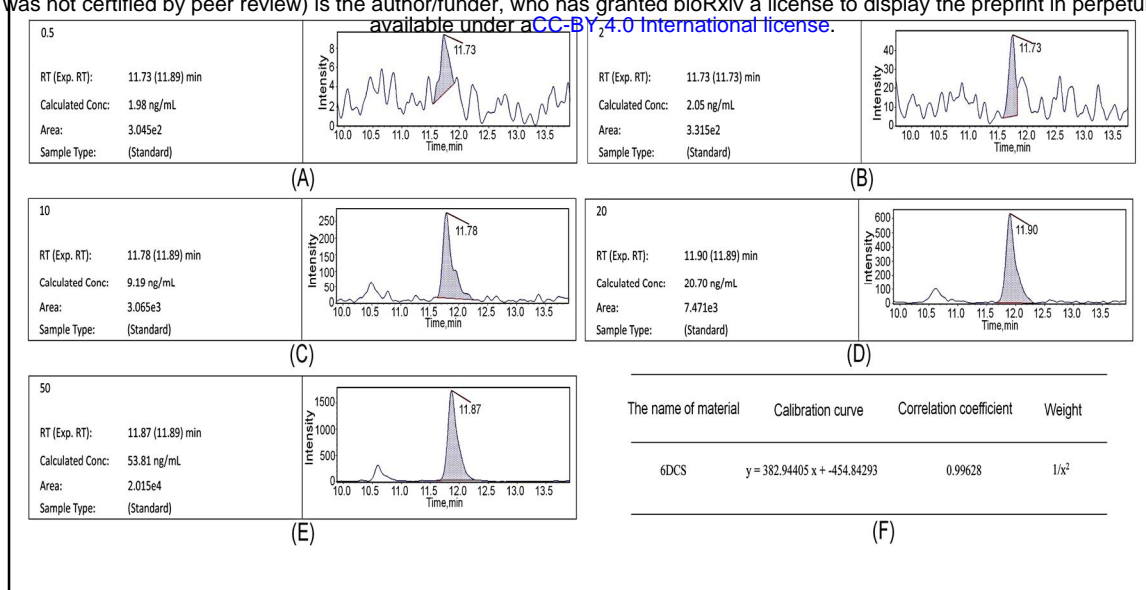


**Supplemental Figure 7 | Chromatogram analyses of tZR standards via HPLC-MS/MS.** The chromatogram of standard tZR at (A) 0.1, (B) 0.2, (C) 0.5, (D) 2, (E) 5, (F) 20, (G) 50, and (H) 200 ng/mL concentrations. (I) Equations for the TZR standard curves.

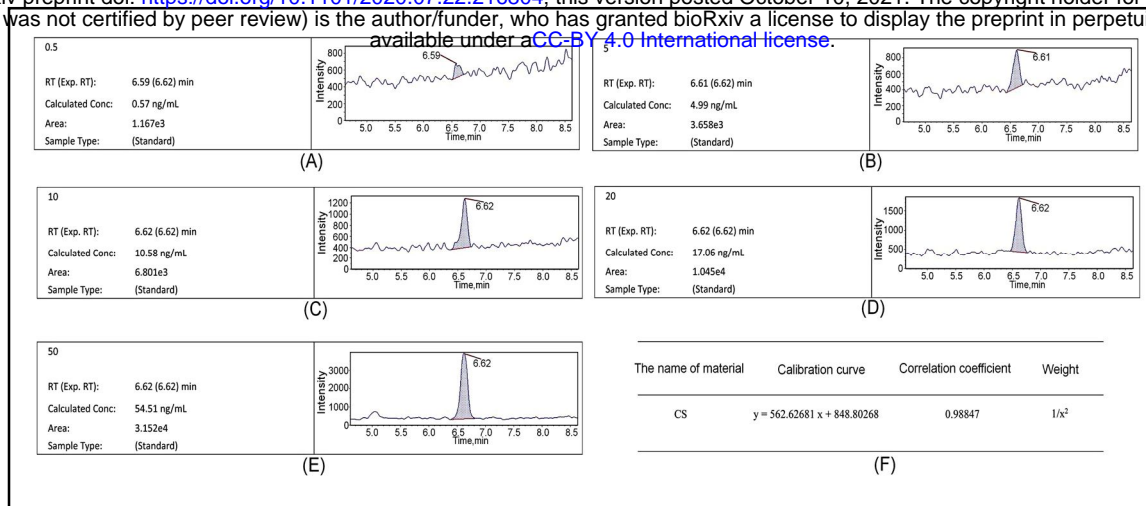




**Supplemental Figure 8 | Chromatogram analyses of IPA standards via HPLC-MS/MS.** The chromatogram of standard IPA at (A) 0.2, (B) 0.5, (C) 2, (D) 5, (E) 20, (F) 50, and (G) 200 ng/mL concentrations. (H) Equations for the IPA standard curves.



**Supplemental Figure 9 | Chromatogram analyses of DCS standards via HPLC-MS/MS.** The chromatogram of standard DCS at (A) 0.5, (B) 2, (C) 10, (D) 20, and (E) 50 ng/mL concentrations. (F) Equations for the DCS standard curves.



**Supplemental Figure 10 | Chromatogram analyses of CS standards via HPLC-MS/MS.** The chromatogram of standard CS at (A) 0.5, (B) 5, (C) 10, (D) 20, and (E) 50 ng/mL concentrations. (F) Equations for the CS standard curves.